

IntechOpen

Clinical Use of Electrocardiogram

Edited by Umashankar Lakshmanadoss



Clinical Use of Electrocardiogram

Edited by Umashankar Lakshmanadoss

Published in London, United Kingdom

Clinical Use of Electrocardiogram

<http://dx.doi.org/10.5772/intechopen.98009>

Edited by Umashankar Lakshmanadoss

Contributors

Illya Chaikovsky, Anatoly Kazmirchik, Sergey Sofienko, You-Bin Liu, Ya-Feng Zhou, Xie Feng, Lin Xu, Yan-Fei Huang, Peter Kupo, Bong Gun Song, N. Devadevi, P. Vijayalakshmi, K. Rajkumar, A. Abiramy Prabavathy, Umashankar Lakshmanadoss, Behram Ahmed Khan

© The Editor(s) and the Author(s) 2023

The rights of the editor(s) and the author(s) have been asserted in accordance with the Copyright, Designs and Patents Act 1988. All rights to the book as a whole are reserved by INTECHOPEN LIMITED. The book as a whole (compilation) cannot be reproduced, distributed or used for commercial or non-commercial purposes without INTECHOPEN LIMITED's written permission. Enquiries concerning the use of the book should be directed to INTECHOPEN LIMITED rights and permissions department (permissions@intechopen.com).

Violations are liable to prosecution under the governing Copyright Law.



Individual chapters of this publication are distributed under the terms of the Creative Commons Attribution 3.0 Unported License which permits commercial use, distribution and reproduction of the individual chapters, provided the original author(s) and source publication are appropriately acknowledged. If so indicated, certain images may not be included under the Creative Commons license. In such cases users will need to obtain permission from the license holder to reproduce the material. More details and guidelines concerning content reuse and adaptation can be found at <http://www.intechopen.com/copyright-policy.html>.

Notice

Statements and opinions expressed in the chapters are these of the individual contributors and not necessarily those of the editors or publisher. No responsibility is accepted for the accuracy of information contained in the published chapters. The publisher assumes no responsibility for any damage or injury to persons or property arising out of the use of any materials, instructions, methods or ideas contained in the book.

First published in London, United Kingdom, 2023 by IntechOpen

IntechOpen is the global imprint of INTECHOPEN LIMITED, registered in England and Wales, registration number: 11086078, 5 Princes Gate Court, London, SW7 2QJ, United Kingdom

British Library Cataloguing-in-Publication Data

A catalogue record for this book is available from the British Library

Additional hard and PDF copies can be obtained from orders@intechopen.com

Clinical Use of Electrocardiogram

Edited by Umashankar Lakshmanadoss

p. cm.

Print ISBN 978-1-80355-528-7

Online ISBN 978-1-80355-529-4

eBook (PDF) ISBN 978-1-80355-530-0

We are IntechOpen, the world's leading publisher of Open Access books Built by scientists, for scientists

6,500+

Open access books available

176,000+

International authors and editors

190M+

Downloads

156

Countries delivered to

Our authors are among the

Top 1%

most cited scientists

12.2%

Contributors from top 500 universities



WEB OF SCIENCE™

Selection of our books indexed in the Book Citation Index
in Web of Science™ Core Collection (BKCI)

Interested in publishing with us?
Contact book.department@intechopen.com

Numbers displayed above are based on latest data collected.
For more information visit www.intechopen.com



Meet the editor



Dr. Umashankar Lakshmanadoss completed his training at the University of Rochester, NY, USA. He served as director of the inpatient medical consult service at Johns Hopkins University School of Medicine, Baltimore, MD, USA, and then joined the Division of Cardiovascular Medicine at Guthrie Clinic, Sayre, PA, USA. Then, he pursued training in cardiac electrophysiology at William Beaumont School of Medicine, Auburn Hills, MI, USA, and continued advanced cardiac electrophysiology training at Mayo Clinic, Rochester, MN, USA. He served as Assistant Professor of Medicine in the Division of Cardiology, Louisiana State University, USA, where he also serves as the director of the complex arrhythmia ablation program. His research interest is cardiac electrophysiology. Currently, Dr. Lakshmanadoss is the director of cardiac electrophysiology at Mercy Health, Cincinnati, OH, USA.

Contents

Preface	XI
Section 1	
Practical Applications of ECG in Arrhythmias	1
Chapter 1	3
Electrophysiology Study: Interpretation of Intracardiac Electrocardiograms <i>by Peter Kupo</i>	
Chapter 2	13
ECG Approach to Narrow QRS Complex Supraventricular Tachycardia <i>by Behram Ahmed Khan and Umashankar Lakshmanadoss</i>	
Chapter 3	27
Electrocardiographic Differential Diagnosis of Narrow QRS and Wide QRS Complex Tachycardias <i>by Bong Gun Song</i>	
Section 2	
Clinical Use of ECG	47
Chapter 4	49
Electrocardiogram and Its Interpretation of Cardiac Diseases in Cattle <i>by N. Devadevi, P. Vijayalakshmi, K. Rajkumar and A. Abiramy Prabavathy</i>	
Chapter 5	61
Unshielded Magnetocardiography in Clinical Practice: Detection of Myocardial Damage in CAD Patients and in Patients Recovered from COVID-19 <i>by Illya Chaikovsky, Anatoly Kazmirchyk, Sergey Sofienko, You-Bin Liu, Ya-Feng Zhou, Xie Feng, Lin Xu and Yan-Fei Huang</i>	

Preface

Cardiovascular disease (CVD) continues to be the leading cause of morbidity and mortality in both developed and developing countries. Early diagnosis and management are key to reducing the number of deaths attributed to CVD. Electrocardiogram (ECG) plays a major role in diagnosing both ischemic heart disease and arrhythmia disorders. Within the context of the current COVID-19 pandemic, related cardiac diseases place additional stress on the health system. Fortunately, CVDs can be diagnosed early via noninvasive techniques. Hence, accurate interpretation of ECG results is vital in cardiology.

This book is divided into two sections on “Practical Applications of ECG in Arrhythmias” and “Clinical Use of ECG.” In cardiac electrophysiology, one of the basic and most important procedures is an electrophysiology study that provides a great amount of information about the electrical system of the heart. In the first section, a chapter is dedicated to the interpretation of intra-cardiac ECG during an electrophysiology study. By obtaining intra-cardiac ECGs, medical professionals can accurately identify and locate arrhythmias, determine the effectiveness of treatments, and guide catheter-based interventions. Two additional chapters in this section discuss the classic ECG features of narrow QRS complex tachycardia and wide QRS complex tachycardia, respectively. It is important to note that differentiating between narrow and wide QRS tachycardia based solely on ECG criteria can sometimes be challenging, and clinical context, patient presentation, and additional diagnostic tests may be required for accurate identification and appropriate management of the tachycardia.

In the second section, one chapter describes the practical applications of ECG in cattle. Another chapter addresses the relationship between COVID-19 infection and acute coronary syndromes, such as myocardial infarction, which can cause direct injury to the heart muscle, leading to myocarditis and myocardial injury. These conditions can result in reduced heart function and an increased risk of developing or exacerbating coronary artery disease (CAD). As such, this section also includes a chapter describing the use of unshielded magnetocardiography in the detection of myocardial damage in patients who are recovering from COVID-19.

I gratefully acknowledge the invaluable organizational skills of the staff at IntechOpen, especially Author Service Manager Ms. Sara Debeuc for her timely and invaluable assistance. I am also thankful to the book’s designer, information technology staff, and marketing representatives who are working to promote the book on various platforms. I sincerely appreciate and applaud all the contributing authors for their excellence, hard work, and commitment to advancing and spreading their knowledge of ECG. They have taken time from their personal and professional life to complete this task. I thank them profusely for that.

This book is dedicated to my little Master Shawn who continues to inspire me and make my life blissful.

We hope that this book will serve as a useful reference for clinical providers interested in comprehensive electrophysiology using intra-cardiac ECGs.

Umashankar Lakshmanadoss, MD, FACC, FHRS
Division of Cardiac Electrophysiology,
The Jewish Hospital of Cincinnati-Mercy Heart Institute,
Cincinnati, OH, USA

Section 1

Practical Applications
of ECG in Arrhythmias

Chapter 1

Electrophysiology Study: Interpretation of Intracardiac Electrocardiograms

Peter Kupo

Abstract

Although electrocardiography is more than 100 years old, it still holds the key to diagnose many disorders and is one of the most commonly used diagnostic tools not only in cardiology but throughout medicine. Most often a surface electrocardiogram (ECG) is made, which represents a summarized electrical activity of the heart. However, by inserting catheters into the heart, it is possible to make an ECG from different localized areas. This chapter focuses on introducing the readers to the world of cardiac electrophysiology providing an overview of the basic principles of the electrophysiology study.

Keywords: cardiac electrophysiology, electrophysiology, EP study, intracardiac electrogram, electrocardiography

1. Introduction

Cardiac electrophysiology study (EPS) is helpful to assess the heart's electrical system. This is an invasive percutaneous cardiac procedure used for the investigation and treatment of certain arrhythmias. During the examination, catheters are inserted to the appropriate position within the heart mainly via large veins to record the electrical signals of the heart and to pace from different localized areas. In this way, EPS can help evaluating the function of the conduction system, determining the mechanisms of brady- and tachyarrhythmias, and identifying areas which may be the targets of often curative catheter ablation. Many cardiac arrhythmias that previously required the use of potentially harmful antiarrhythmic drugs can now be routinely cured in the electrophysiology laboratory by means of transcatheter ablation techniques.

In this chapter, the basics of cardiac electrophysiological studies are presented.

2. Principles of the electrophysiology study

2.1 The setup of the electrophysiology study

Equipment necessary for EPS includes an operation table, fluoroscopy unit, recorders, programmable stimulator, a multichannel lead switching box, an

oscilloscope, and emergency instruments. In addition, tools for vascular access and electrode catheters are also required [1]. A standard schematic set-up for typical EPS is shown in **Figure 1**.

2.2 Signal recording, amplification, and filtering

Electrical signals from humans obtained by surface or intracardiac electrodes are <10 mV in amplitude. These electrocardiograms must be amplified and filtered before digitalization, displaying, and storage for interpretation and analysis [2]. Amplification means the increase of the signal's amplitude. However, the signals are plagued with electrical noise, thus amplification results in increasing not only the original signals but the amplitude of noise also. For this reason, avoidance of extraneous signals is essential: all electrical tools used in EPS should be appropriately earthed and shielded. In addition, filtering is required to eliminate unnecessary components of the electrical signals. High-pass filters remove components below a given frequency, while low-pass filters eliminate high-frequency components of the electrical signal. Electrophysiological signals are often contaminated with power line noise (i.e., 60 Hz in North America and 50 Hz in Europe), thus notch filtering is often used to eliminate it [3].

Standard ECG devices run at 25 mm/s. Increasing the paper output speed, subtle ECG findings hidden in the tracings become more evident. During an EPS, surface ECG leads and intracardiac electrocardiograms (IEGM) are generally displayed and interpreted at a sweep speed of 100 or 200 mm/s (**Figure 2**).

2.3 Standard catheter positions

For a standard EPS, a standard number of four catheters is necessary. Based on the operator's decision, EPS is also feasible using only three diagnostic catheters. Diagnostic catheters have two or multiple electrodes, and for each pair of consecutive electrodes, a distinct intracardiac electrogram gets recorded. Traditionally, catheter placement is carried out under fluoroscopy guidance. In the EP lab, three main

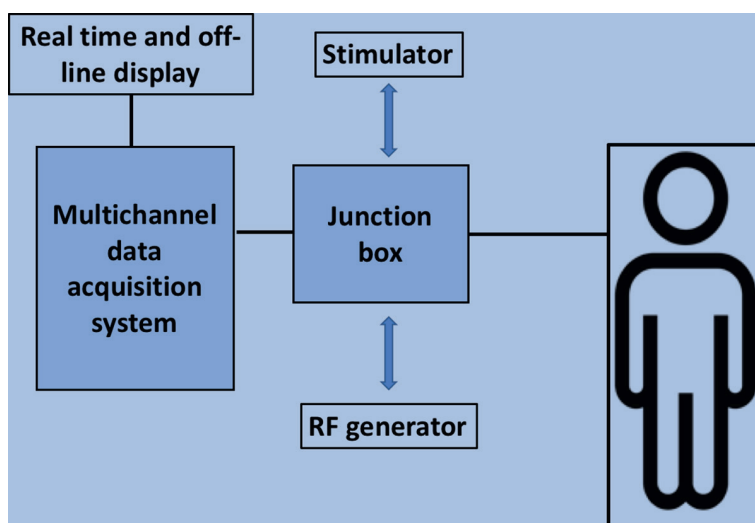


Figure 1. Standard schematic set-up for typical electrophysiology study. Abbreviation: RF—radiofrequency.

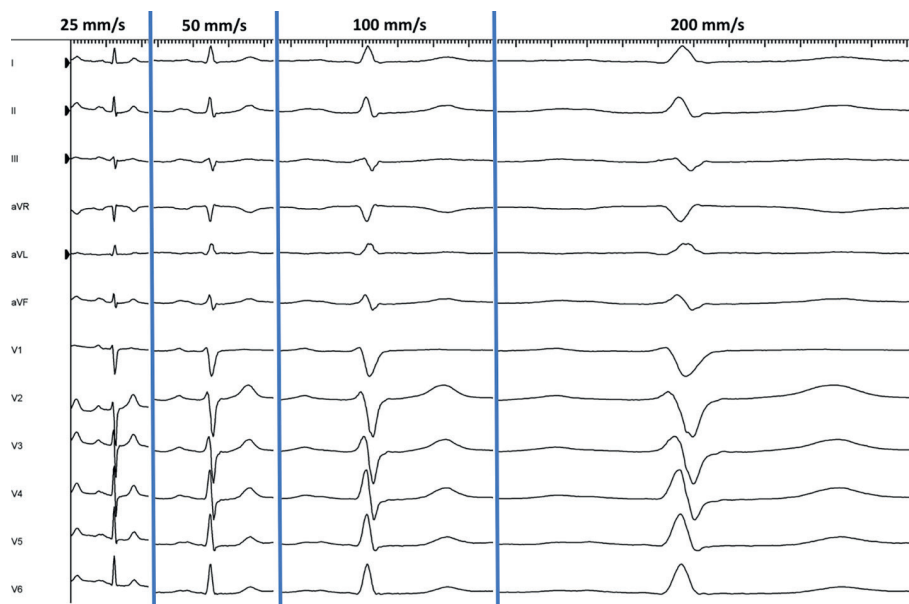


Figure 2.
Same normal sinus beat at a paper speed of 25, 50, 100, and 200 mm/s.

fluoroscopy projections are used: anteroposterior (AP), left anterior oblique (LAO), and right anterior oblique (RAO) views (**Figure 3**).

2.3.1 High right atrium

A diagnostic catheter is positioned from the femoral vein and contacted with the lateral wall of the right atrium at right atrium—superior vena cava junction.

2.3.2 Coronary sinus

The coronary sinus runs transversely in the left atrioventricular groove on the posterior side of the heart. A multielectrode catheter is inserted into the coronary sinus

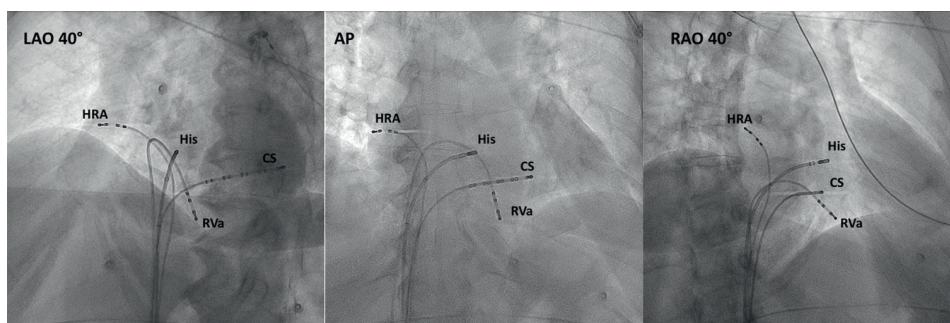


Figure 3.
Standard catheter positions in left anterior oblique (LAO), anteroposterior (AP), and right anterior oblique (RAO) projections. Abbreviations: CS—coronary sinus decapolar catheter; HRA—high right atrium; RVa—right ventricle apex.

from femoral, jugular internal, or subclavian vein. For femoral approach, steerable catheters are used. CS catheter allows to record IEGMs coming from the left atrium and ventricle. Moreover, this position is easily reproducible and serves as a reference point during the EPS. Thus, CS catheters play an important role in EP labs.

2.3.3 His bundle

For recording His bundle electrogram, a catheter is inserted via femoral vein to the high septal part of the right ventricle and pulled back slowly with clockwise torquing till characteristic His bundle electrogram appears.

2.3.4 Right ventricular apex

A diagnostic catheter is advanced from femoral vein to apical right ventricle, which allows to record local ventricular IEGMs.

2.4 Introduction to evaluate intracardiac electrocardiograms, basic intervals

Generally, IEGMs mean the electrical activity between two electrodes at the tip of the catheter (bipolar recording) [4]. The main difference between surface ECG and IEGMs is that the surface ECG records a summation of the electrical activity of the heart, while in contrast, IEGMs show only the electrical activity of a localized area, i.e., IEGMs are local intracardiac electrograms. Importantly, these are displayed together on the monitor system facilitating accurate interpretations of the electrical signals (**Figure 4**).

After catheter placement, a routine EPS starts with the measurement of basic intervals [4]. Ideally basic intervals should be measured during sinus rhythm.

2.4.1 PA interval

The PA interval represents the interval between the earliest atrial activation (recording in any channel) in the region of the sinus node and at the region of the atrioventricular node. Usually, the earliest atrial activation is represented by the P wave onset on the surface ECG. Normal value is 25–55 milliseconds (ms).

2.4.2 AH interval

AH interval represents the conduction time from the low-right atrium at the interatrial septum through the atrioventricular (AV) node to the His bundle. It is measured between the atrial electrogram recorded by the His bundle catheter and the beginning of the His electrogram itself. The normal range is 55–150 ms [4]. The AH interval is sensitive to autonomic tone. A prolonged AH interval may indicate AV nodal disease or high vagal tone, whereas a shorter than normal AH can occur during sympathetic activation.

2.4.3 HV interval

HV interval reflects conduction through the His-Purkinje system and is measured on the His bundle electrogram from the beginning of the His deflection to the earliest identified ventricular activity on the surface ECG. An HV interval of 35–55 ms is

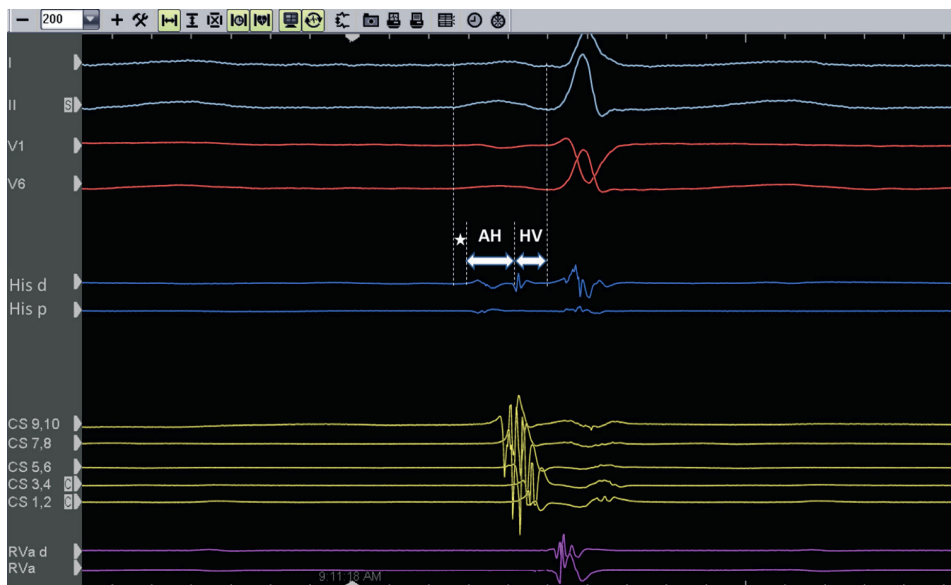


Figure 4. Snapshot from an electrophysiology study. The upper four channels represent lead I, II, V₁, and V₆ of surface ECG. The paper speed is 200 mm/s. on the distal His (His d) channel, we can recognize three different wavefront characteristics of the His bundle: the first one is the A (atrial) wave (synchronous to P wave on surface ECG), the last is called V (ventricular) wave (synchronous to QRS complex on the surface ECG). In the middle, a sharp signal represents His bundle electrogram. AH interval could be measured from the beginning of A to the sharp His signal. HV interval is measured on the His bundle electrogram from the beginning of the His deflection to the earliest identified ventricular activity on the surface ECG. CS electrograms show atrial activation (synchronous to P wave on surface ECG again). Note that first activation occurs on CS 9,10 which is the proximal pair of electrodes. CS 9,10 is at the ostium of the coronary sinus, thus these electrodes are the closest to the sinus node. In the case of a correctly positioned CS catheter, CS 9,10 should be activated first during normal sinus rhythm. Finally, a local ventricular electrogram can be easily identified on the catheter at RVa position. Asterix represents PA interval.

considered normal. In the presence of anterograde conducting accessory pathway, the HV interval may be shorter. Prolonged HV interval represents infrahisian conduction disturbances.

2.5 Time measurement and pacing

2.5.1 Cycle length

Time measurements are reported in milliseconds in the case of EP procedures. To characterize the heart rate, the cycle length (CL) is used instead of the frequency. CL represents the length of time between each atrial or ventricular beats. For example, a tachycardia with a heart rate of 150 beats per minute has a CL of 400 ms (**Figure 5**). The faster the heart rate the shorter the CL.

2.5.2 Pacing

Besides IEGM recordings, electrode catheters previously inserted in the heart are also used for pacing. An external stimulator is connected to the catheters. When pacing starts, electrical current is passed by catheters resulting in cardiac cells'

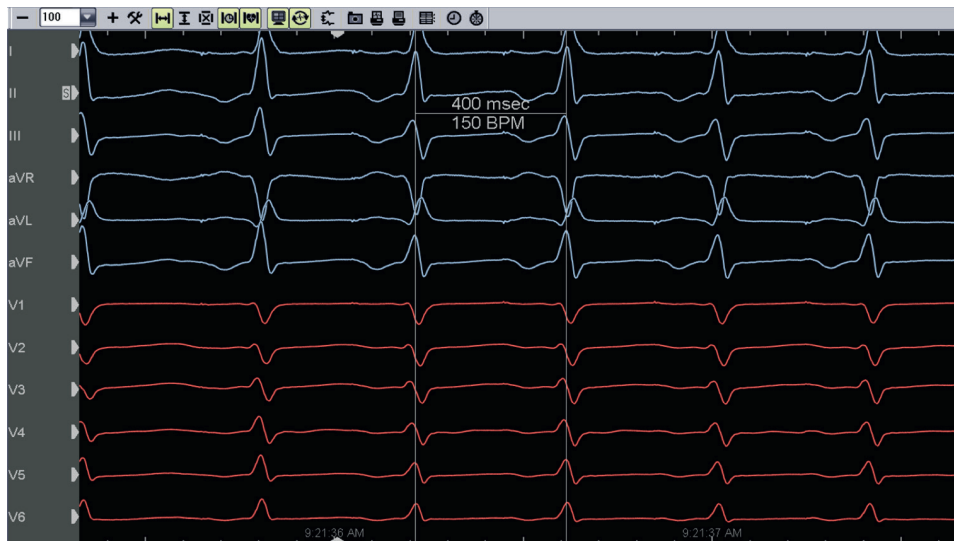


Figure 5. Atrial pacing at a cycle length of 400 ms, which means a rate of 150 beats per minute. Sharp pacing artifacts are present before P waves. P waves are negative in the inferior leads (pacing from coronary sinus ostium). Paper speed is 100 mm/s.

depolarization near the catheter's electrode. The depolarization of these cells generates an electrical wavefront, spreading over the heart as the impulse originating from the sinus node. As a result, stimulator pacing generates cardiac impulse artificially. Carefully positioned catheters can impulse the heart from almost any position. During the EPS, pacing is used to introduce electrical impulses in predetermined patterns and at precise time intervals. Such pacing is called programmed stimulation [1]. Programmed stimulation consists of the main type of pacing technique: burst and extrastimulus pacing.

2.5.2.1 Burst pacing

Burst pacing consists of implementing a series of electrical impulses (so-called drive train) at a fixed cycle length. By definition, each impulse is called S1 and the difference between the impulses is the same (**Figure 6**).

2.5.2.2 Extrastimulus testing

Extrastimulus testing means introduction of a drive train (usually 8 beats, S1) followed by one or more extrastimuli with shorter coupling interval than the cycle length of the drive. S2 means the first programmed extrastimulus, S3 is used for the second, and so on (**Figure 7**).

2.6 Measurement of refractory periods

During EPS, refractory periods of cardiac tissues can be characterized by measuring effective, functional, and relative refractory periods [5].



Figure 6. Ventricular burst pacing from RVa position. Note the pacing artifact on RVa channel and before the QRS complexes. Pacing cycle length is fixed (500 ms). Paper speed is 50 mm/s.



Figure 7. Atrial extrastimulus testing from coronary sinus catheter (CS). The drive train consists of 8 beats at a cycle length of 400 ms is followed by an extrastimulus with a shorter coupling interval (300 ms). Ablation catheter (ABL) is in the His region showing His bundle electrogram. Paper speed is 50 mm/s.

2.6.1 Effective refractory period

Most commonly used as it is part of a routine EPS. It represents the longest coupling interval that fails to capture the tissue or be conducted over the structure (**Figure 8**).

2.6.2 Functional and relative refractory period

A routine EPS does not include the measurements of the functional and relative refractory period. Functional refractory period means the lower limit shortest “output” coupling interval that can be produced by any “input” interval. Relative

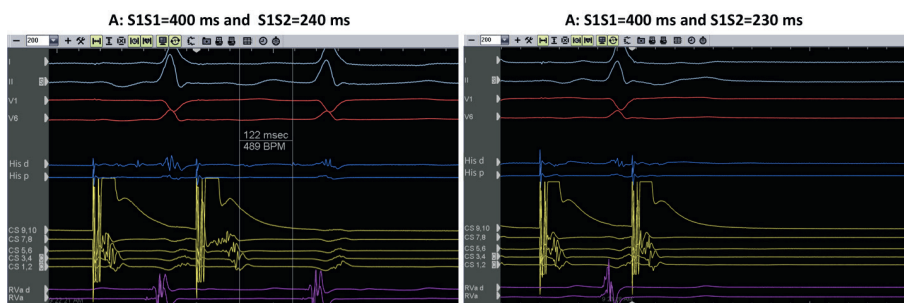


Figure 8. Programmed atrial stimulation from CS 9,10. Drive cycle length is 400 ms. Panel A shows ventricular contraction (i.e., QRS complex) after S₂ extrastimulus at a coupling interval of 240 ms. However, Panel B represents atrioventricular block after S₂ extrastimulus at a coupling interval of 230 ms. In this case, effective refractory period of the AV node (AVNERP) is 230 ms.

refractory periods represent the point at which latency begins to occur. RRP means “input” interval to a tissue at which the “output” interval just begins to differ from the “input” interval.

3. Summary

This chapter summarized the basics of electrophysiological studies of the heart. The author sincerely hopes that the chapter may have contributed to a deeper understanding of the world of electrocardiograms.

Conflict of interest


The author declares no conflict of interest.

Author details

Peter Kupo
Heart Institute, Medical School, University of Pécs, Pécs, Hungary

*Address all correspondence to: peter.kupo@gmail.com

IntechOpen

© 2022 The Author(s). Licensee IntechOpen. This chapter is distributed under the terms of the Creative Commons Attribution License (<http://creativecommons.org/licenses/by/3.0>), which permits unrestricted use, distribution, and reproduction in any medium, provided the original work is properly cited. 

References

- [1] Fogoros RN. Principles of the EP study. In: Fogoros RN, editor. *Fogoros' Electrophysiologic Testing*. 5th ed. Hoboken, New Jersey, USA: Wiley-Blackwell; 2015
- [2] Venkatachalam KL, Herbrandson JE, Asirvatham SJ. Signals and signal processing for the electrophysiologist: Part II: Signal processing and artifact. *Circulation. Arrhythmia and Electrophysiology*. 2011;4:974-981
- [3] Murgatroyd F, Krahn AD. The electrophysiology laboratory. In: Murgatroyd F, Krahn AD, editors. *Handbook of Cardiac Electrophysiology*. London, United Kingdom: Remedica; 2002
- [4] Issa ZF, Miller JM, Zipes DP. Electrophysiological testing: Tools and techniques. In: Issa ZF, Miller JM, Zipes DP, Murgatroyd F, Krahn AD, editors. *Clinical Arrhythmology and Electrophysiology*. 3rd ed. New York, NY, USA: Elsevier; 2019
- [5] Murgatroyd F, Krahn AD. The basic electrophysiology study. In: Murgatroyd F, Krahn AD, editors. *Handbook of Cardiac Electrophysiology*. London, United Kingdom: Remedica; 2002

Chapter 2

ECG Approach to Narrow QRS Complex Supraventricular Tachycardia

Behram Ahmed Khan and Umashankar Lakshmanadoss

Abstract

Supraventricular tachycardia (SVT) is an irregular heart rhythm in which the focus of impulse lies above the bundle of His, i.e., the sinus node, the atria, and the atrioventricular node (AVN). There are two types of SVT: Narrow QRS complex tachycardia and wide QRS complex tachycardia. Narrow QRS complex tachycardias can further be divided as regular or irregular based on R–R intervals. There is further classification that can be made in regular rhythms in terms of RP interval. The most common tachycardias that are characterized by a long RP interval include sinus tachycardia, atrial tachycardia, and atrioventricular reentrant tachycardia. Short RP interval tachycardias mainly Atrioventricular nodal reentrant tachycardia (AVNRT), junctional tachycardia (JT) and permanent junctional reciprocating tachycardia (PJRT). On the other hand, irregular SVTs usually include atrial fibrillation, atrial flutter, and multifocal atrial tachycardia.

Keywords: Supraventricular tachycardia, Narrow QRS complex tachycardia, Wide QRS complex tachycardia, Atrioventricular reentrant tachycardia, Junctional rhythm, Permanent junctional reciprocating tachycardia, Atrial fibrillation

1. Introduction

Supraventricular tachycardia (SVT) is a type of arrhythmia that originates from areas above the bundles of His, i.e., the sinus node, atria, and atrioventricular node (AVN), manifesting with heart rate > 100 beats/min. In terms of duration, it can be sustained, non-sustained (<30 seconds), paroxysmal, and persistent. Tachycardias are usually classified according to anatomical structure like atrial, AV nodal, and due to accessory pathway. Nonetheless, since an electrocardiogram (ECG) is used for diagnosis, it is better to approach the diagnosis and classify SVTs according to the characteristics of the ECG. Generally, SVTs fall into two categories; narrow QRS complexes and wide QRS complexes. This chapter will focus on ECG approach to narrow QRS complex SVTs, **Figure 1**.

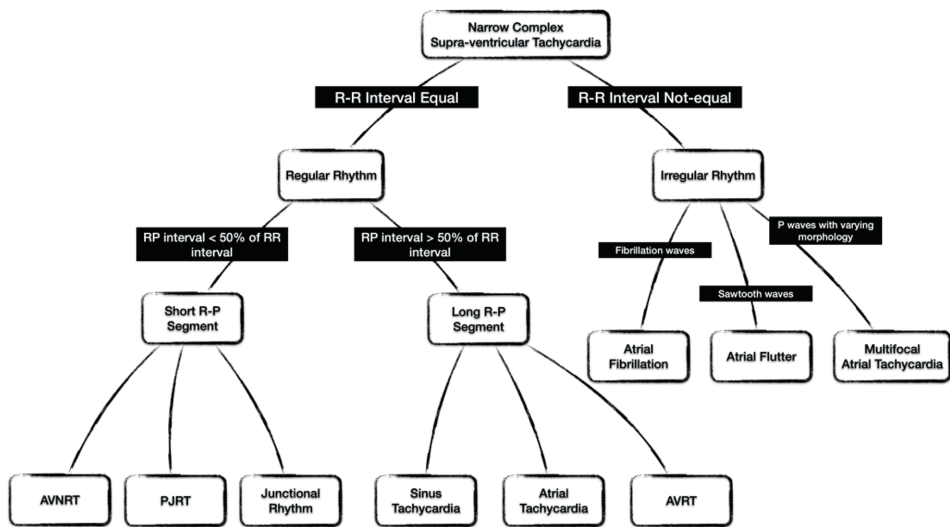


Figure 1.
Algorithm to define the supraventricular tachycardia.

1.1 Narrow QRS complex supraventricular tachycardia

While approaching an SVT, the first step would be to determine whether it's a narrow or wide QRS complex. If the QRS complex is <120 ms (<3 small boxes on the ECG) it is narrow complex and it is >120 ms (>3 small boxes on the ECG) it is defined as wide QRS complex.

1.2 Regular rhythm vs. irregular rhythm

The next step would be to determine if the rhythm is regular or irregular. The RR interval can be used to decide if the rhythm is regular or irregular ECG. If the rhythm is regular,

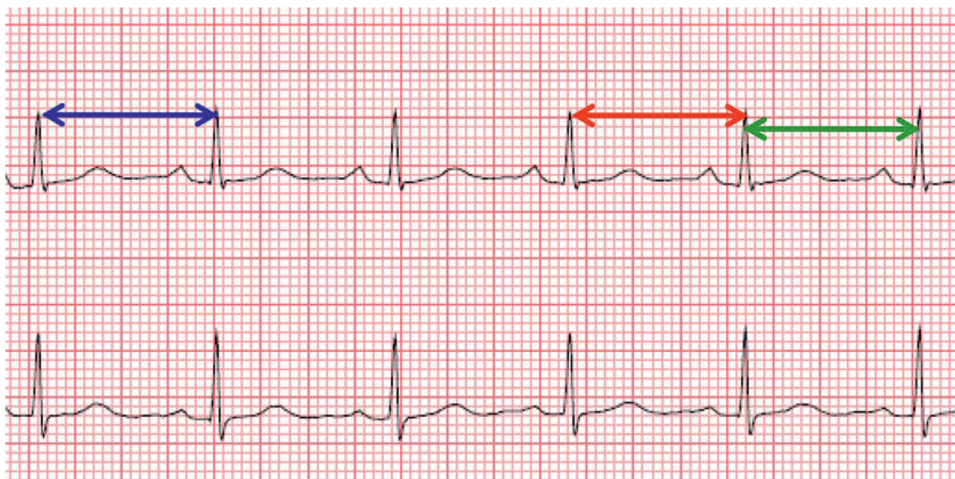


Figure 2.
Regular RR interval. The length of blue, red and green arrows are equal showing the regularity of the RR interval.



Figure 3. Irregular RR interval. The length of blue, red and green arrows are not equal showing the irregularity of the RR interval.

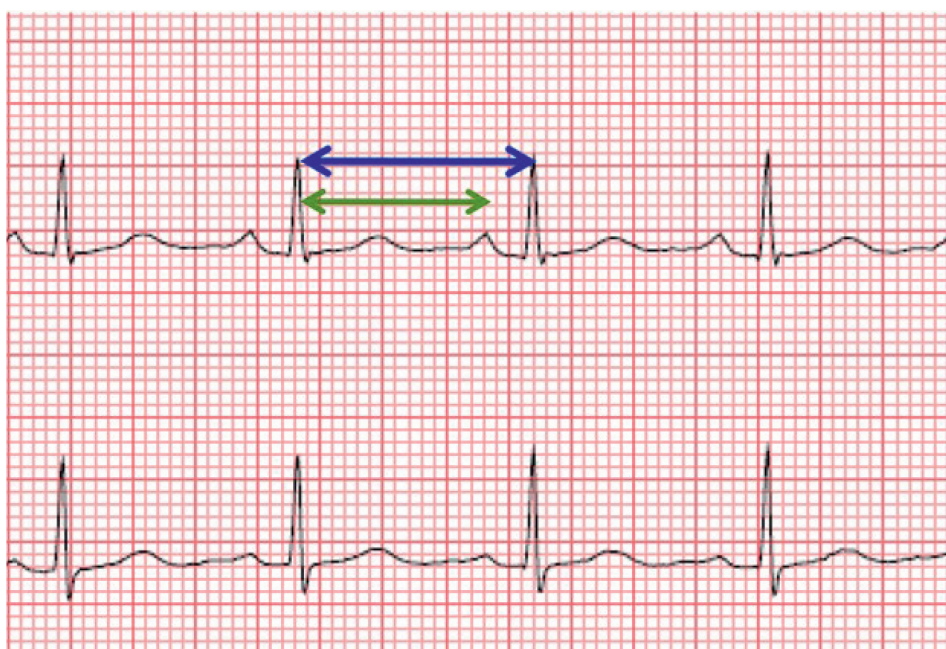


Figure 4. Long RP interval. The RP interval (green arrow) is more than half of RR interval (blue arrow).

the RR intervals will be equal, but if it is irregular, the RR intervals will be anything but equal. If the RR interval is regular, it's a regular narrow QRS complex rhythm, **Figure 2**. If the RR interval is irregular, it's an irregular narrow QRS complex rhythm, **Figure 3**.

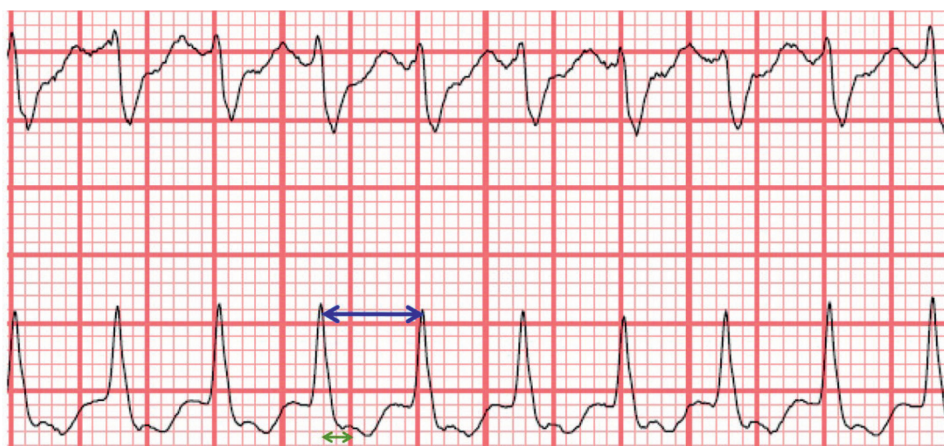


Figure 5.
Short RP interval. The RP interval (green arrow) is less than half of RR interval (blue arrow).

1.3 Long RP interval vs. short RP interval

The third step would be to determine the RP interval. SVT can be classified into two categories based on RP interval: Short RP (RP interval less than half of RR interval) and long RP (RP interval greater than half of RR interval) **Figures 4 and 5**. The RP interval is defined as the time interval between ventricular and atrial activation. On an ECG, an RP interval is the distance between the onset of the QRS complex and the end of the P wave. An approximate assumption would be that rhythms which originate from the AV node or perinodal tissue have a short RP interval and rhythms that originate elsewhere would have a long RP interval.

2. Regular rhythm

2.1 Sinus tachycardia

2.1.1 Narrow QRS complex, regular rhythm with long RP interval

In general, sinus tachycardia occurs as an appropriate response of the body to stress (illness, exercise, pulmonary embolism, hypovolemia, pain) or as a pathological abnormality of the SA node (sinus node re-entry tachycardia) [1]. Typically in this type of arrhythmia, there is an increased rate of firing of the SA node. This is demonstrated by an impulse that starts from the SA node and moves to the right atrium then to the left atrium and finally reaching the AV node, **Figure 6**.

Approach to ECG findings: Heart rate > 100 (total R waves on long lead \times 6) \rightarrow Narrow QRS complex (QRS < 120 ms) \rightarrow Regular RR intervals (RR intervals are equal) \rightarrow Long RP interval (RP interval > half of RR interval) \rightarrow Upright P wave in leads I, II and aVL (showing sinus origin), and a negative P wave in lead aVR.

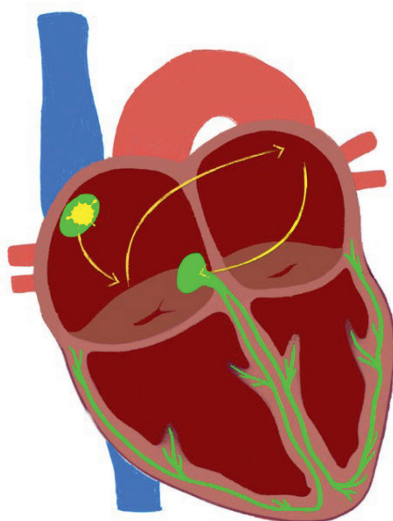


Figure 6.
The impulse is generated in the sinus node (yellow drop sign), followed by a normal conduction pathway to the atria (yellow arrow) and ultimately to the AVN.

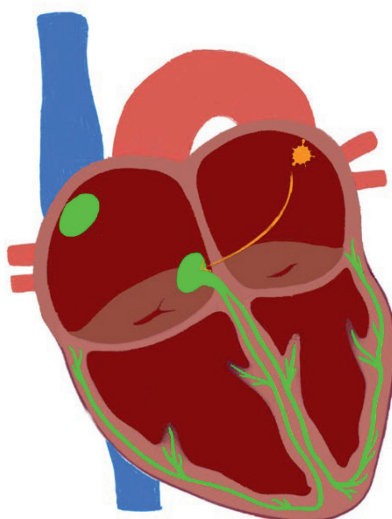


Figure 7.
An impulse is generated in the atria but not in the sinus node (the orange drop signs), which travels to the AVN.

2.2 Atrial tachycardia (focal atrial tachycardia)

2.2.1 Narrow QRS complex, regular rhythm with long RP interval

The term atrial tachycardia, also known as atrial ectopic tachycardia, refers to an arrhythmia that originates from an atrial site other than the SA node and it is

commonly paroxysmal in nature. Focal atrial tachycardia (Focal AT) is relatively uncommon, accounting for between 5% – 15% of arrhythmias in adults [2]. The most common sites of activation are the crista terminalis, tricuspid annulus, and pulmonary vein. Atrial myocytes (any focal site) are activated (either by an automatic, triggered, or micro-reentrant event) and spread centrifugally to reach the AV node, **Figure 7** [3].

Approach to ECG findings: Heart rate > 100 (total R waves on long lead × 6) → Narrow QRS complex (QRS < 120 ms) → Regular RR intervals (RR intervals are equal) → Long RP interval (RP interval > half of RR interval) → if origin is near SA node, there will be an upright P wave in leads I, II and aVL and a negative P wave in lead aVR.

It is important to compare the P wave morphology with the previous ECG, particularly in leads V1 and II, to be able to differentiate the etiology. Secondly, even though focal ATs are regular, the heart rate may increase in the first few beats of the tachycardia and gradually decelerate in the last few beats (warming up phenomenon). Notably, if there is an abrupt onset or termination of the AT (e.g., over a period of three to four beats), it is more suggestive of focal atrial tachycardia [4].

Moreover, it can be diagnosed with the greatest degree of accuracy if two or more of the following findings are present: (a) RP/PR ratio ≥ 1.65 , (b) no P waves in inferior leads, and (c) P wave duration >96 ms [5].

Using the following approach, it is possible to determine the location of the focus of AT as well [6].

- A. If there is a negative or biphasic P wave in V1 with an initially positive deflection and a terminally negative deflection, then the AT focus is probably in the right atrium, not the left atrium.
- B. If there is a biphasic P wave in V1 with an initial negative/terminally positive deflection, it is likely that the AT focus is paraseptal in nature.
- C. A positive P wave in V1 indicates that there is an AT focus in the left atrium.

2.3 Atrioventricular reentrant tachycardia

2.3.1 Narrow QRS complex, regular rhythm with long RP interval

Atrioventricular reentrant tachycardia (AVRT) is an anatomically defined reentrant tachycardia characterized by the presence of the normal AV conduction system and the accessory AV pathway. Atrial premature beats initiating an orthodromic AVRT are blocked in the accessory pathway but conduct antegrade to the ventricles over the AV node/His-Purkinje system. As the impulse is conducted through the ventricles, it then travels back via the AV accessory pathway into the atria in a retrograde fashion. This completes the reentrant loop, **Figure 8** [7]. This reentrant loop leads to tachycardia.

Approach to ECG findings: Heart rate > 100 (total R waves on long lead × 6) → Narrow QRS complex (QRS < 120 ms) → Regular RR intervals (RR intervals are equal) → Long RP interval (RP interval > half of RR interval).

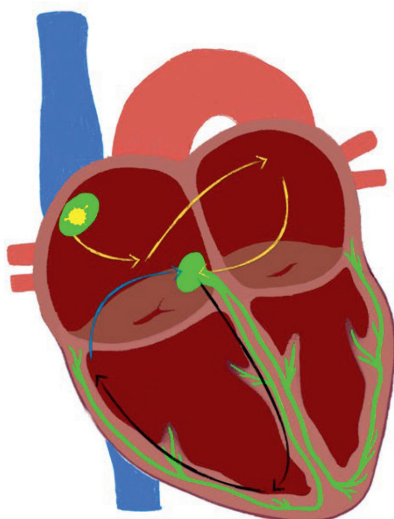


Figure 8.
An accessory pathway (blue arrow) and the AV node form a reentrant circuit.

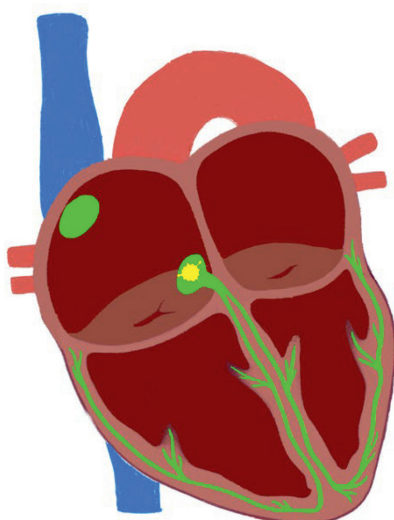


Figure 9.
AV node (yellow drop sign) generates impulses at a higher rate than sinus node.

2.4 Junctional rhythm

2.4.1 Narrow QRS complex, regular rhythm with short RP interval

As the name implies, an accelerated junctional rhythm (JR) occurs when the rate of an AV junctional pacemaker exceeds the rate of the sinus node. In this situation,

an increase in automaticity in the AV node occurs in conjunction with a decreasing amount of automaticity in the sinus node (**Figure 9**). There is a possibility that the retrograde impulse from the AV node may suppress the SA node.

Approach to ECG findings: Heart rate > 100 (total R waves on long lead \times 6) \rightarrow Narrow QRS complex (QRS < 120 ms) \rightarrow Regular RR intervals (RR intervals are equal) \rightarrow Short RP interval (RP interval < half of RR interval) \rightarrow Retrograde P waves may be present and appear before, during or after the QRS complex.

There are usually inverted P waves in inferior leads (II, III, aVF), upright P waves in aVR and V1. If the SA node is not suppressed by retrograde AV impulses, AV dissociation may be present with the ventricular rate usually greater than the atrial rate [8].

2.5 Permanent junctional reciprocating tachycardia

2.5.1 Narrow QRS complex, regular rhythm with short RP interval

This type of tachycardia is also dependent upon the accessory pathway. As the AV node is responsible for generating impulses, these impulses are transmitted retrogradely through the accessory pathways to the atria. This results from characteristically slow conduction of the accessory pathway in permanent junctional reciprocating tachycardia (PJRT) in contrast to AVRT which has a “fast” accessory pathway, **Figure 10**.

Approach to ECG findings: Heart rate > 100 (total R waves on long lead \times 6) \rightarrow Narrow QRS complex (QRS < 120 ms) \rightarrow Regular RR intervals (RR intervals are equal) \rightarrow Long RP interval (RP interval > half of RR interval).

Retrograde P waves may be present and appear before, during or after the QRS complex. There are usually inverted P waves in inferior leads (II, III, aVF), upright P waves in aVR and V1. If the SA node is not suppressed by retrograde AV impulses, AV dissociation may be present with the ventricular rate usually greater than the atrial rate.

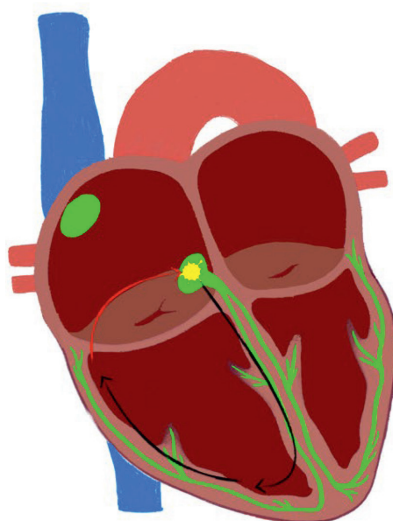


Figure 10.
Slow accessory pathways (red arrow) and the AV node form a reentrant circuit.

2.6 Atrioventricular nodal reentrant tachycardia

2.6.1 Narrow QRS complex, regular rhythm with short RP interval

Atrioventricular nodal reentrant tachycardia (AVNRT) is a regular tachycardia resulting from a reentry circuit that occurs inside the atrium and perinodal tissue. AVNRT is a paroxysmal regular tachycardia characterized by two electrical pathways (fast and slow) near or inside the AV node, **Figure 11**. Fast pathways conduct quickly and exhibit a relatively long refractory period. In contrast, the slow pathway conducts relatively slowly and has a shorter refractory period [9, 10].

Approach to ECG findings: Heart rate > 100 (total R waves on long lead \times 6) \rightarrow Narrow QRS complex (QRS < 120 ms) \rightarrow Regular RR intervals (RR intervals are equal) \rightarrow Short RP interval (RP interval < half of RR interval).

If P waves are visible, they exhibit retrograde conduction with P wave inversion in leads II, III, and aVF. They may be buried within the QRS complex, visible afterward, or appear before the QRS. There will be pseudo S wave in Lead II and pseudo R wave in V1.

3. Irregular rhythm

3.1 Atrial fibrillation

Atrial fibrillation is one of the most common supraventricular tachycardias it is characterized by chaotic rapid atrial electrical activity with and without variable ventricular rate, **Figure 12**. Its pathophysiology usually varies depending upon the type of atrial fibrillation. Ectopic foci are generally the cause of paroxysmal atrial fibrillation, whereas sustained atrial fibrillation is caused by arrhythmogenic substrates formed by fibrosis of myocytes and arrhythmogenic stimulation by triggers [11].

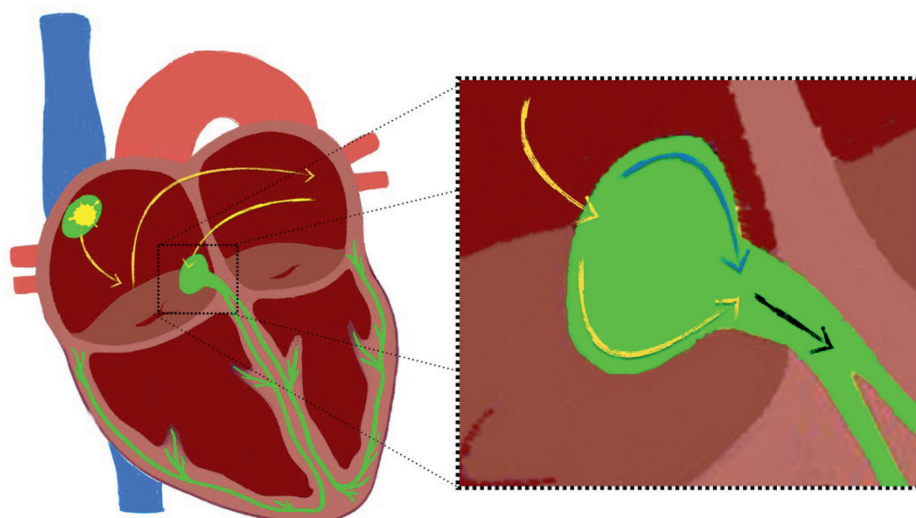


Figure 11. A reentrant circuit forms through the normal fast atrioventricular nodal conduction pathway (yellow drop sign) and the slow perinodal accessory pathway (blue arrow).

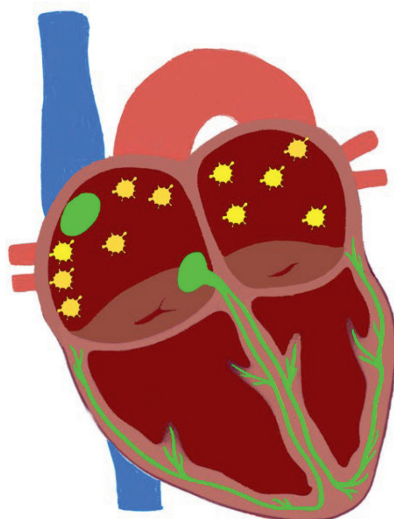


Figure 12.
Atrial tissue generates multiple impulses in a chaotic manner (yellow drop signs).

Approach to ECG findings: Heart rate > 100 (total R waves on long lead \times 6) \rightarrow Narrow QRS complex (QRS < 120 ms) \rightarrow Irregular RR intervals (RR intervals are not equal). There is no distinct presence of P waves, however chaotic fibrillation waves could be seen.

3.2 Multifocal atrial tachycardia

Multifocal atrial tachycardia (MAT) is an uncommon SVT characterized by an irregular rhythm and discrete P waves with varying morphologies, which are often observed in patients with pulmonary disease during acute exacerbations of the disease. It is the most common arrhythmia to be confused with atrial fibrillation due to varying morphology of the P waves. An increased intracellular calcium store is thought to trigger the arrhythmia from different atrial locations, which may occur as a consequence of hypokalemia, hypoxia, acidemia, and increased catecholamines, **Figure 13** [12].

Approach to ECG findings: Heart rate > 100 \rightarrow Narrow QRS complex (QRS < 120 ms) \rightarrow Irregular RR intervals (RR intervals are not equal) \rightarrow discrete P waves with at least three different morphologies (including the sinus P wave).

3.3 Atrial flutter with or without variable block

An atrial flutter, also known as macro-reentrant atrial tachycardia, is caused by macro reentrant circuits within the annulus of the tricuspid valve with impulse conduction along the Cavo-tricuspid isthmus, **Figure 14**. It is possible for this macro reentrant circuit to be found in other areas of the atria. Therefore, it can be a typical atrial flutter (through the Cavo-tricuspid isthmus) or an atypical atrial flutter (in another part of the atria). Usually, this circuit develops as a result of fibrosis of atrial myocytes. There is an organized atrial activity, which is commonly observed as sawtooth flutter waves with a rate exceeding 200 beats per minute. Atrial flutter may manifest as an irregular SVT if there is a variable block, however it may also manifest as a regular SVT if there is no variable block.

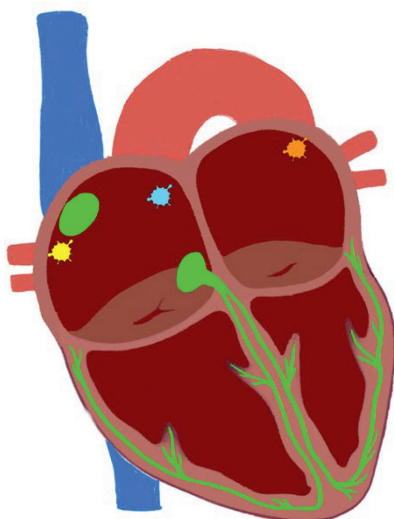


Figure 13.
The atrial tissue (drop signs) generates impulses in different places.

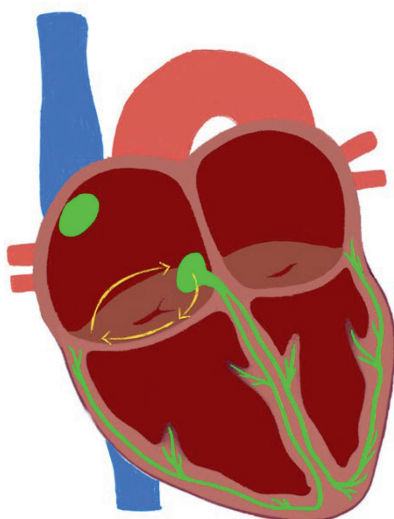


Figure 14.
A macro-reentrant circuit develops along the Cavo-tricuspid isthmus (yellow arrows).

Approach to ECG findings: Heart rate > 100 (total R waves on long lead \times 6) \rightarrow Narrow QRS complex (QRS < 120 ms) \rightarrow Irregular RR intervals (RR intervals are not equal) \rightarrow QRS complex is preceded by multiple P waves (two to three sawtooth-like waves) within a single lead with the same morphology. When the circuit is counterclockwise, it produces negative sawtooth flutter waves in leads II, III, and aVF. When the direction of the circuit is reversed, a positive P wave is produced in leads II, III, and aVF [13].

4. Conclusion

Generally, ECG findings are used to determine the type of SVT. This four-step approach can be used to identify SVTs 1. Determine if the QRS complex is narrow or wide; 2. Determine whether the rhythm is regular or irregular; 3. If the rhythm is regular, determine whether the RP interval is short or long; 4. Analyze the P wave for presence, morphology, and regularity to define supraventricular arrhythmias.

Conflict of interest

The authors declare no conflict of interest.

Author details


Behram Ahmed Khan^{1*} and Umashankar Lakshmanadoss²

1 The Jewish Hospital of Cincinnati-Mercy Health, Cincinnati, Ohio, USA

2 The Jewish Hospital of Cincinnati-Mercy Heart Institute, Cincinnati, Ohio, USA

*Address all correspondence to: behramkhanmd@outlook.com

IntechOpen

© 2023 The Author(s). Licensee IntechOpen. This chapter is distributed under the terms of the Creative Commons Attribution License (<http://creativecommons.org/licenses/by/3.0>), which permits unrestricted use, distribution, and reproduction in any medium, provided the original work is properly cited. 

References

- [1] Yusuf S, Camm AJ. The sinus tachycardias. *Nature Clinical Practice. Cardiovascular Medicine*. 2005;2(1):44-52
- [2] Chen SA et al. Sustained atrial tachycardia in adult patients. Electrophysiological characteristics, pharmacological response, possible mechanisms, and effects of radiofrequency ablation. *Circulation*. 1994;90(3):1262-1278
- [3] Page RL et al. 2015 ACC/AHA/HRS Guideline for the management of adult patients with supraventricular tachycardia. *Circulation*. 2016;133(14):e506-e574
- [4] Saoudi N et al. A classification of atrial flutter and regular atrial tachycardia according to electrophysiological mechanisms and anatomical bases; a Statement from a Joint Expert Group from The Working Group of Arrhythmias of the European Society of Cardiology and the North American Society of Pacing and Electrophysiology. *European Heart Journal*. 2001;22(14):1162-1182
- [5] Yagishita A et al. Differentiation of atrial tachycardia from other long RP tachycardias by electrocardiographic characteristics. *Journal of Arrhythmia*. 2014;30(5):376-381
- [6] Kistler PM et al. P-wave morphology in focal atrial tachycardia: development of an algorithm to predict the anatomic site of origin. *Journal of the American College of Cardiology*. 2006;48(5):1010-1017
- [7] Akhtar M et al. Electrophysiologic mechanisms of orthodromic tachycardia initiation during ventricular pacing in the wolff-parkinson-white syndrome. *Journal of the American College of Cardiology*. 1987;9(1):89-100
- [8] Gibler WB. Foreword. In: Chan TC et al, editors. *ECG in Emergency Medicine and Acute Care*. Mosby: Philadelphia; 2005. pp. xiii-xiv
- [9] Moe GK, Preston JB, Burlington H. Physiologic evidence for a dual A-V transmission system. *Circulation Research*. 1956;4(4):357-375
- [10] Mazgalev TN, Tchou PJ. Surface potentials from the region of the atrioventricular node and their relation to dual pathway electrophysiology. *Circulation*. 2000;101(17):2110-2117
- [11] Bosch NA, Cimmini J, Walkey AJ. Atrial Fibrillation in the ICU. *Chest*. 2018;154(6):1424-1434
- [12] Lee Scher D, Arsura EL. Multifocal atrial tachycardia: mechanisms, clinical correlates, and treatment. *American Heart Journal*. 1989;118(3):574-580
- [13] Daoud EG, Morady F. Pathophysiology of atrial flutter. *Annual Review of Medicine*. 1998;49:77-83

Chapter 3

Electrocardiographic Differential Diagnosis of Narrow QRS and Wide QRS Complex Tachycardias

Bong Gun Song

Abstract

Narrow QRS complex tachycardias or Wide QRS complex tachycardias are common problems encountered in clinical practices. Although such tachycardias often occur in patients with a normal anatomy and/or function of heart and rarely represent life-threatening conditions, they are common sources of morbidity and/or mortality. Narrow QRS complex tachycardias are fast cardiac rhythms with QRS duration of 120 ms or less while wide QRS complex tachycardias are fast cardiac rhythms with QRS duration of 120 ms or more. Origins of narrow QRS complex tachycardias are above or within the His bundle. Wide QRS complex tachycardias can be ventricular tachycardias, supra-ventricular tachycardias with bundle branch block or accessory pathway. The purpose of this chapter is to present the differential diagnosis of narrow and wide QRS complex tachycardias.

Keywords: narrow QRS tachycardia, wide QRS tachycardia, tachycardia, electrocardiograms, regular rhythm NCTs, irregular rhythm NCTs

1. Introduction

Differential diagnosis and treatment of tachycardias is a common dilemma encountered by physicians or cardiologists. Although such tachycardias often occur in patients with a normal heart, they may cause bothersome symptoms and rarely represent life-threatening conditions. Among these tachycardias with a heart rate greater than 100 beats per minute (bpm), the narrow QRS complex tachycardias (NCTs) are defined by the presence in a 12-lead electrocardiogram (ECG) of a QRS complex duration less than 120 ms and the wide QRS complex tachycardias (WCTs) are defined by the presence in a 12-lead ECG of a QRS complex duration more than 120 ms (**Figure 1**) [1–10]. The NCTs are typically of supraventricular origin above or within the His bundle, although rarely narrow complex ventricular tachycardias (VT) have been reported in the literature in which early activation of the His bundle can also occur in high septal VT, resulting in relatively narrow QRS complexes of 110–140 ms (**Table 1**, [1–5]). The WCTs can be VT or supraventricular tachycardia (SVT) with right or left bundle branch block (BBB) or right or left accessory pathway (**Table 1**, [6–10]). Because administration of medications based on misdiagnosis of these tachycardias can be harmful and sometimes fatal, diagnosis

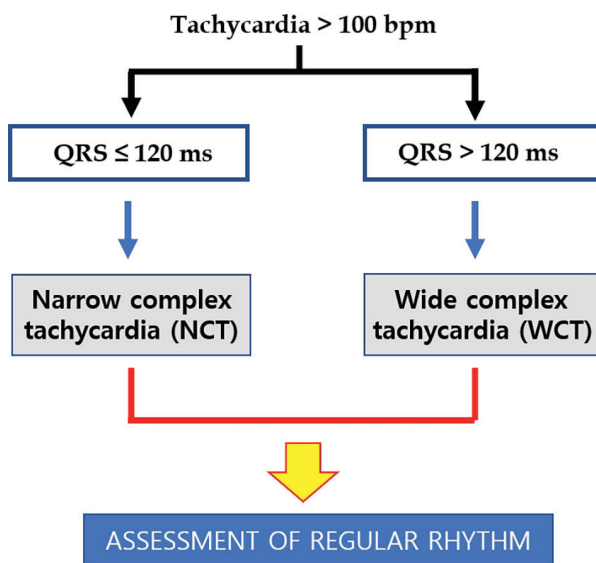


Figure 1.
Differential diagnostic algorithm of NCTs and WCTs.

The NCTs with QRS duration less than 120 ms	The WCTs with QRS duration more than 120 ms
<i>Regular rhythm</i>	<i>Regular rhythm</i>
<ul style="list-style-type: none"> • Sinus tachycardia • Sinus node reentrant tachycardia • Atrial tachycardia • Atrial flutter • Junctional tachycardia • Paroxysmal SVT (AVNRT / Orthodromic AVRT) • Permanent junctional reciprocating tachycardia (PJRT) 	<ul style="list-style-type: none"> • VT/Ventricular flutter • Antidromic AVRT • SVT with aberrant conduction / BBB • Atrial tachycardia with accessory pathway • Junctional tachycardia with accessory pathway
<i>Irregular rhythm</i>	<i>Irregular rhythm</i>
<ul style="list-style-type: none"> • Atrial tachycardia with variable AV conduction • Multifocal atrial tachycardia (MAT) • Atrial flutter with variable AV conduction • Atrial fibrillation 	<ul style="list-style-type: none"> • Polymorphic VT / Ventricular fibrillation • Antidromic AVRT with variable VA conduction • Pre-excited AF • Torsades de pointes • AF or atrial flutter or focal atrial tachycardia with varying block conducted with aberration

SVT; supra-ventricular tachycardia, AVNRT; atrio-ventricular nodal re-entrant tachycardia, AVRT; atrio-ventricular reciprocating tachycardia, AV; atrio-ventricular, VT; ventricular tachycardia, BBB; bundle branch block, AF; atrial fibrillation, VA; ventriculo-atrial.

Table 1.
Differential diagnosis of NCTs and WCTs.

of these tachycardias is critical [11–13]. The accurate, rapid diagnosis in patients with these tachycardias still remains a significant clinical dilemma, because the published numerous ECG algorithms and criteria are complicated and difficult to recall in urgent clinical situations [11–13]. We have reviewed ECG findings of the NCTs and WCTs in order to reduce the possible diagnostic errors on the ECGs.

2. NCTs

The NCTs are common problems encountered in clinical situations [1–5, 14–21]. The key to approaching the diagnosis of these arrhythmias is identifying atrial activity (P waves) on the ECG and classifying these tachycardias according to the presence of AV dissociation (**Figure 2**) and then re-classifying according to long RP or short RP (**Table 2**) [1–5, 14–21]. On the basis of these algorithm, a differential diagnosis can

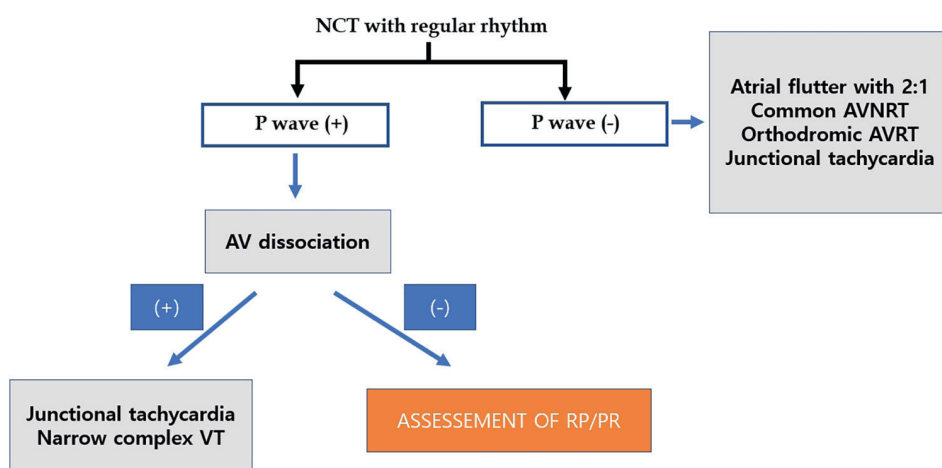


Figure 2.
 Differential diagnostic algorithm of NCTs with regular rhythm.

Short RP (RP < PR)	Long RP (RP > PR)
• AVNRT	• Sinus tachycardia
• AVRT	• Sinus nodal reentrant tachycardia
• Junctional tachycardia	• Atrial tachycardia
	• Junctional tachycardia
	• PJRT
	• AVNRT (unusual type, fast-slow)
	• AVRT (atypical type)

AVNRT; atrio-ventricular nodal re-entrant tachycardia, AVRT; atrio-ventricular reciprocating tachycardia, PJRT; Permanent junctional reciprocating tachycardia.

Table 2.
 Differential diagnosis of NCTs according to RP interval.

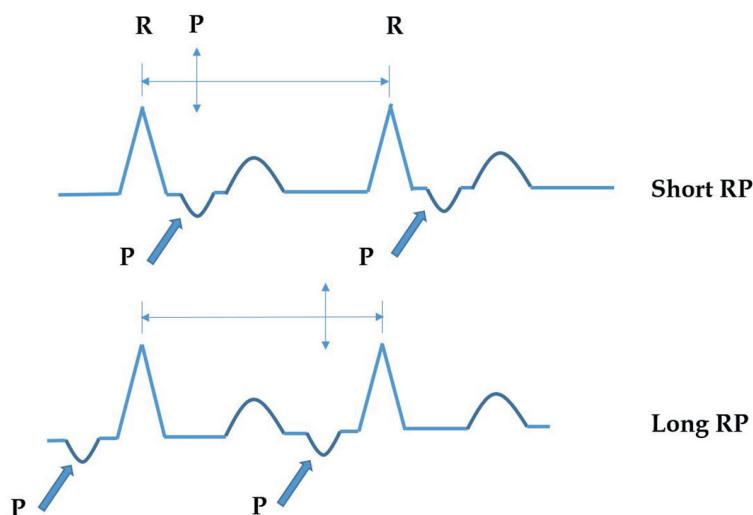


Figure 3.
Schematic demonstration of short RP and long RP.

be generated, logical therapy can be delivered for termination of the tachycardia, and a plan can be developed to prevent recurrence.

Short RP tachycardias are defined as regular tachycardias in which interval from QRS complex to P wave (upper arrows, **Figure 3**) much less than interval from P wave to subsequent QRS complex, whereas long RP tachycardias are defined as regular tachycardias in which interval from QRS complex to P wave much more than interval from P wave to subsequent QRS complex (lower arrows, **Figure 3**) [1–5, 14–21].

2.1 NCTs with regular rhythm

2.1.1 Sinus tachycardia

Sinus tachycardia is defined as an increase in sinus rate to more than 100 bpm with regular rhythm. The rate increases gradually and may show beat to beat variation. Although generally identifiable by a P wave of normal morphologic features that precedes each QRS complex, sinus tachycardia can be difficult to recognize when the P wave begins to fuse with the T wave of the preceding QRS complex. Sinus tachycardia is usually a physiological response such as fever, anxiety, pain, hyperthyroidism but may be precipitated by sympathomimetic drugs or endocrine disturbances [5, 14–21].

2.1.2 Sinus nodal reentrant tachycardia

The morphologic appearance of sinus nodal reentrant tachycardia is identical to that of sinus tachycardia. In contrast to sinus tachycardia, the rate is very regular and initiation and termination are abrupt without an underlying physiological stimulus. Vagal maneuver may be successful in stopping the arrhythmia [5, 14–21].

2.1.3 Atrial tachycardia

Atrial tachycardia (AT) is usually a NCTs accounting for 5–15% of SVT. Other than sinus tachycardia, AT is the most common long RP tachycardia. In AT, an atrial source

outside the sinoatrial node due to focal automatic activity or re-entry circuit activates the atria. Accordingly, P-wave morphologic characteristics vary depending on the site of this source. Digitalis toxicity should be suspected in patients with paroxysmal AT with AV block [5, 14–22].

2.1.4 Atrial flutter

Atrial flutter is a reentrant rhythm of the right atrium typically with an atrial rate of 250 to 350 beats/min. The flutter may circulate in a counterclockwise direction around the tricuspid annulus in the frontal plane (typical, counterclockwise flutter) or in a clockwise direction (atypical, clockwise flutter). P waves have a characteristic “sawtooth” appearance, and 2:1 AV block is common. Because one flutter wave occurs in the ST-T segment and another flutter wave occurs before each QRS complex in atrial flutter with 2:1 AV conduction, atrial flutter is neither a short RP nor a long RP tachycardia [5, 14–22].

2.1.5 Junctional tachycardia

Non-paroxysmal junctional tachycardia (NPJT) is a tachycardia that arises in the AV junction. Although often described as a short RP tachycardia, because NPJT causes ventricular activation almost concurrently with atrial activation, a substantial portion (25%), which is described as a long RP tachycardia, actually show P waves that slightly precede the QRS complex. and in some cases, AV dissociation may be present. Unlike AVNRT and AVRT, initiation and termination are gradual. NPJT is often associated with digitalis intoxication, inferior myocardial infarction, myocarditis, and mitral valve surgical procedures [5, 14–23].

2.1.6 Paroxysmal SVT (AVNRT/Orthodromic AVRT)

2.1.6.1 AVNRT

AV nodal reentrant tachycardia (AVNRT) is characterized by a tachycardia with supraventricular origin, with sudden onset and termination generally at rates between 150 and 250 beats/min and is the most common cause of SVT except atrial fibrillation, atrial flutter, and sinus tachycardia. In majority of patients (noted as the “typical” or “slow-fast” AVNRT), anterograde conduction to the ventricle occurs over the “slow” pathway and retrograde conduction to the atrium occurs over the “fast” pathway and the atria are activated either simultaneously with or just after activations of the ventricles and this common type is classified as a short RP tachycardia. Rarely, in “atypical” or “fast-slow” AVNRT, the reentry occurs in the opposite direction in which anterograde conduction occurs over the “fast” pathway, while retrograde conduction occurs over “slow” pathway, and this rare type is classified as a long RP tachycardia [24–31].

2.1.6.2 AVRT

AV reentrant tachycardia (AVRT) involves reentry between the atria and ventricles with use of the AV node–His bundle conduction as the anterograde and slow pathway and an accessory conduction as the retrograde and fast pathway. This pattern is also known as orthodromic reciprocating tachycardia (ORT). This type is not apparent by analysis of the ECG during sinus rhythm because the ventricle is not pre-excited and

the accessory pathway is said to be “concealed”. In tachycardia, retrograde conduction over the accessory pathway is fast and yields a short RP tachycardia [24–31].

In contradistinction to ORT resulting in NCTs, antidromic AVRT has anterograde conduction over the accessory pathway and retrograde conduction over the AV node-His bundle resulting in WCTs [24–31].

The following factors are important differences between AVNRT and AVRT [24–31]:

In contradistinction to AVNRT, an 1:1 relationship is necessary for AVRT because both the atria and the ventricles are part of the reentry circuit. Therefore, if AV block occurs during tachycardia, AVRT is excluded.

If bundle branch block occurs during ORT and the length of the tachycardia cycle increases, AVNRT is excluded because the His-Purkinje system is not part of the tachycardia reentry circuit in AVNRT. The converse is not necessarily true because the absence of cycle length change with the occurrence of bundle branch block does not exclude AVRT.

2.1.7 Permanent junctional reciprocating tachycardia (PJRT)

As discussed with AVRT, certain types of reentrant circuits exist in which the accessory AV connection has AV nodal properties such as slow conduction. In PJRT, excitation over the postero-septal accessory pathway conducts very slowly, because of a long and tortuous route of pathway. Tachycardia is maintained by anterograde AV nodal conduction and retrograde conduction over slow accessory pathway. Because of slow conduction property of accessory pathway, retrograde atrial activation is delayed, and a long RP tachycardia results. Patients with this type of accessory pathway almost never have preexcitation (a delta wave) on ECGs during sinus rhythm [5, 14–23].

2.2 NCTs with irregular rhythm

2.2.1 Atrial tachycardia with variable AV conduction

Atrial tachycardia with atrioventricular block is typically seen with digoxin toxicity. The ventricular rhythm is usually regular but may be irregular if atrioventricular block is variable [5, 14–21].

2.2.2 Multifocal atrial tachycardia (MAT)

MAT is characterized by P waves with variable morphologies and variable PR intervals. Differential diagnosis between MAT and atrial fibrillation can be possible by the presence of isoelectric baselines between the P waves in MAT. MAT is seen typically in patients with chronic obstructive pulmonary disease or digoxin toxicity [5, 14–21, 32].

2.2.3 Atrial flutter with variable AV conduction

Atrial flutter is due to a re-entry circuit in the right atrium with secondary activation of the left atrium. This produces atrial contractions at a rate of about 300 beats/min as flutter (F) waves. F waves show broad and saw-tooth appearances and are best seen in lead V1 and the inferior leads [5, 14–21].

2.2.4 Atrial fibrillation

This is the most common sustained arrhythmia with overall prevalence is 1% to 1.5%. Atrial fibrillation is caused by multiple re-entrant circuits or “wavelets” of activation sweeping around the atrial myocardium without effective atrial contraction. Atrial fibrillation is seen on the ECG as irregular baseline undulations of variable amplitude and morphology (called f waves) discharging at a frequency of 350 to 600 beats/min.

With normal conduction, ventricular rate shows frequency between 100 and 150 beats/min. Atrial fibrillation with slow ventricular responses or AV block is seen typically in patients with digoxin toxicity [5, 14–21, 33–36].

3. WCTs

3.1 WCTs with regular rhythm

3.1.1 VT/ventricular flutter

Monomorphic ventricular tachycardia is common in patients with a history of previous myocardial infarction. Other rare causes of monomorphic VT include right or left ventricular outflow tract ventricular tachycardia and right ventricular dysplasia.

Ventricular flutter appears as a sine wave pattern with regular, large oscillations on the ECG and can progress to ventricular fibrillation [37–44].

3.1.2 Antidromic AVRT

Antidromic AVRT includes a reentrant circuit with accessory pathway as the antero-grade pathway, and AV node–His bundle as the retrograde pathway. Some patients (3 to 8%) with WPW syndrome show mechanisms of antidromic AVRT [24–31].

- SVT with aberrant conduction/BBB
- Atrial tachycardia with accessory pathway
- Junctional tachycardia with accessory pathway

3.2 WCTs with irregular rhythm

3.2.1 Polymorphic VT/ventricular fibrillation

Polymorphic VT is most commonly caused by abnormalities of ventricular muscle repolarization. The predisposition to this problem usually manifests on the ECG as a prolongation of the QT interval. Congenital problems include long QT syndrome and catecholaminergic polymorphic ventricular tachycardia. Acquired problems are usually related to drug toxicity or electrolyte abnormalities, myocardial ischemia. Class III anti-arrhythmic drugs such as sotalol and amiodarone prolong the QT interval and may in some circumstances be pro-arrhythmic. Other relatively common drugs include some antibiotics and antihistamines [37–44].

Ventricular fibrillation is a terminal arrhythmia in which ventricular contractions are uncoordinated and too weak to eject blood. The ECG shows irregular, chaotic deflections of varying amplitude and shape [37–44].

- Antidromic AVRT with variable VA conduction
- Pre-excited AF (AF with ventricular pre-excitation)
- Torsades de pointes

The ECG demonstrates a polymorphic VT characterized by the QRS complexes of changing amplitude that appear to twist around the isoelectric line and occur at the rates of 200 to 250 beats/min. Most data suggest that early afterdepolarizations are responsible for both the QT prolongation and the torsades de pointes. The most common causes are congenital severe bradycardia, potassium depletion and use of class IA and IC drugs. Clinical features depend on whether torsades de pointes is due to acquired or congenital long QT syndrome. Some episodes may persist and progress to ventricular fibrillation, leading to sudden death. In congenital long QT syndrome, long QT intervals predispose the patient to an R-on-T phenomenon, wherein the R-wave, representing ventricular depolarization, occurs during the relative refractory period at the end of repolarization [37–44].

- AF or atrial flutter or focal atrial tachycardia with varying block conducted with aberration

4. ECG criteria favoring ventricular rather than supra-ventricular tachycardia in WCTs

There are several algorithms that are currently used to help distinguish Supraventricular Tachycardia (SVT) with aberrancy and Ventricular Tachycardia (VT) (Table 3). Many of these algorithms and criteria have limitations [44–49, 50–64].

4.1 Sandler and Marriott criteria (1965)

[RBBB morphology] Identical activation vector = SVT.

If the initial 20 ms of the QRS are the same in WCT as in sinus rhythm, SVT is favored with a positive predictive value (PPV) of 92%. The sinus rhythm ECG must be available for this analysis.

[RBBB morphology] An rSR' where S crosses baseline = SVT with a PPV of 91%.

[RBBB morphology] Triphasic QRS in V1 = SVT with a PPV of 92%.

[RBBB morphology, LBBB morphology] Precordial concordance = VT. A QRS, which is predominantly positive or predominantly negative in every precordial lead, overwhelmingly favors VT with specificity of 95–100% and a PPV of 89–100% [44–49, 50–65].

4.2 Wellens criteria of right bundle branch block

AV dissociation = VT. Of all criteria, this is the most secure with specificity of 100% and PPV of 100%. It holds true regardless of bundle branch pattern or other morphology criteria.

QRS duration	
<ul style="list-style-type: none"> • > 160 ms with LBBB pattern or > 140 ms with RBBB pattern • QRS duration during tachycardia is narrower than in sinus rhythm 	
QRS axis	
<ul style="list-style-type: none"> • Right superior (northwest) axis • RBBB pattern with left axis deviation • RBBB pattern with normal axis • LBBB pattern with right axis deviation • QRS axis shift >40 degrees between sinus rhythm and tachycardia 	
Precordial QRS concordance	
Positive or negative concordance in all precordial leads	
AV dissociation	
<ul style="list-style-type: none"> • AV ratio < 1 • VA ratio > 1 (VA block) • Fusion beats • Capture beats 	
RBBB morphology	
Lead V1	Lead V6
<ul style="list-style-type: none"> • mono or biphasic QRS • R, qR, Rs, broad R • Triphasic QRS (Rsr' ['Rabbit ears']) 	<ul style="list-style-type: none"> • R/S < 1, QS, QR, monophasic R
LBBB morphology	
Lead V1–2	Lead V6
<ul style="list-style-type: none"> • Initial r wave ≥ 40 ms • Onset of QRS to S nadir interval ≥ 70 ms • Notching on the downstroke of S wave 	<ul style="list-style-type: none"> • Any Q wave (QR, QS) (Absence of Q wave favors SVT)
Initial R wave (+) in lead aVR	
R wave peak time in lead II ≥ 50 ms	
$V_i/V_t \leq 1$	
<i>RBBB; right bundle branch block, LBBB; left bundle branch block, SVT; supra-ventricular tachycardia.</i>	

Table 3.
 ECG criteria favoring ventricular rather than supra-ventricular tachycardia in WCTs.

[RBBB morphology] QRS duration >140 ms = VT with specificity of 57–75% and PPV of 89%.

[RBBB morphology] Left axis deviation = VT with PPVs of 88–94%. With extreme left axis (more negative than -90°), the PPV is 98%.

[RBBB morphology] Mono- or biphasic QRS morphologies in V1 favors VT with PPV of 82–83%.

If the V1 QRS is triphasic, an R:S ratio < 1 in V6 (that is, R wave smaller than S wave) favors VT with PPV of 90%.

[RBBB morphology] Rsr' ('Rabbit ears') = VT. In an unusual triphasic V1, with the left R wave taller than the right, and the S wave not crossing the baseline, favors VT with PPV of 100% [44–49, 50–64].

4.3 Griffith criteria

A history of myocardial infarction, QRS morphology in leads aVF and V1 ([1] predominant negative deflection in aVF in tachycardia with RBBB pattern and Q wave, [2] a monophasic or biphasic waveform in V1 in tachycardia with RBBB pattern, [3] QS or qR waveform in tachycardia with LBBB pattern favored a diagnosis of VT) and frontal plane axis $> 40^\circ$ when compared with baseline the ECG favored a diagnosis of VT. The presence of AV dissociation and/or the presence of premature ventricular beats during sinus rhythm that show morphologies same to that observed in tachycardia favored a diagnosis of VT [50–64, 66–68].

4.4 Kindwall criteria of left bundle branch block (LBBB)

[LBBB morphology] V1 or V2 with initial R > 30 ms = VT.

[LBBB morphology] V1 or V2 QRS onset to nadir of S wave > 60 ms = VT.

[LBBB morphology] V1 or V2 with notching on the S wave downstroke = VT.

[LBBB morphology] Any Q in V6 = VT [50–64, 69].

4.5 Pava criteria using the measurement of the R-wave peak time (RWPT) in lead II

An R-wave peak time, with the interval from QRS onset to first change in polarity (R or S peak) in lead II ≥ 50 ms, independent of whether the complex is positive or

RWPT in lead II algorithm

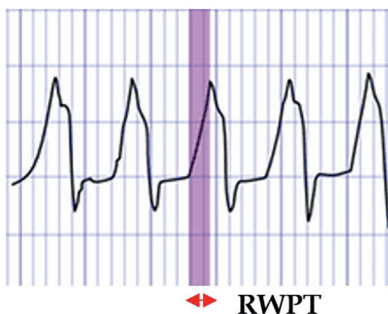
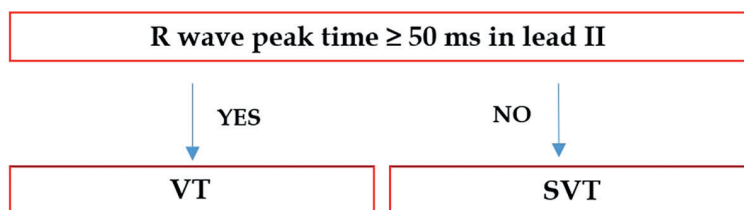


Figure 4.
The R-wave peak time (RWPT) in lead II.

Vereckei aVR algorithm

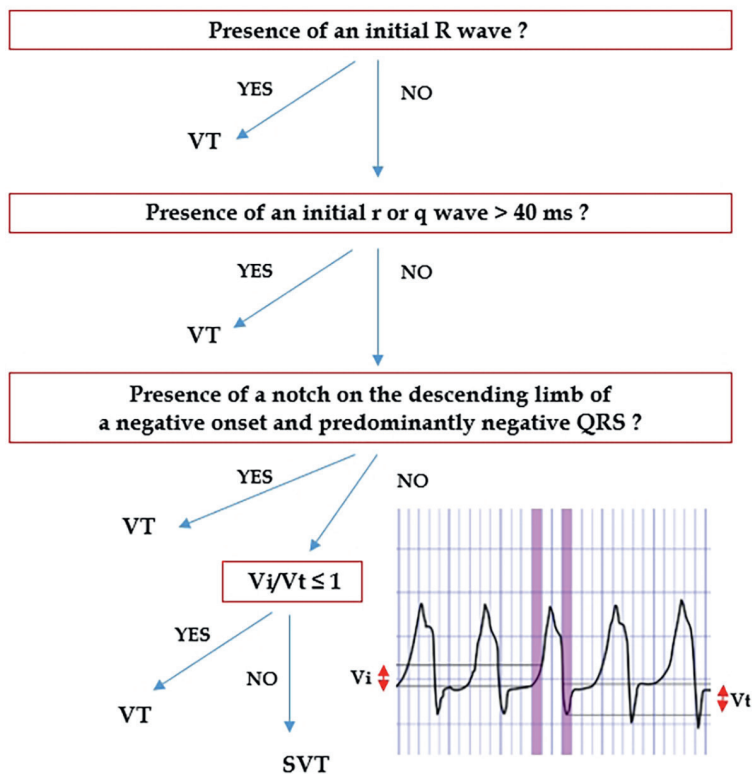


Figure 5.
Vereckei aVR algorithm.

negative, has been reported to have a sensitivity of 93% and specificity of 99% for identifying VT (Figure 4) [50–64, 70].

4.6 Vereckei aVR algorithm

Vereckei et al. published four-step algorithms with the incorporation of new criteria of V_i/V_t (Figure 5) [50–64, 71].

The four steps were used in the following sequence:

1. If an initial R wave was present in lead aVR, VT was diagnosed.
2. If an initial, non-dominant q or r in aVR > 40 ms, VT was diagnosed.
3. If the morphology of WCT did not correspond to BBB or fascicular block, VT was diagnosed.
4. In the last step when the V_i/V_t ratio, obtained by measuring the voltage of the initial 40 ms (V_i) and the terminal 40 ms of a QRS (V_t) in any ECG lead, was ≤ 1 the diagnosis of VT, if the V_i/V_t was >1 the diagnosis of SVT was made (Figure 5).

During WCT due to SVT, after the initial rapid septal activation over the normal His-Purkinje system, the slow intraventricular activation occurs in the mid to terminal portion of the QRS, thus the $V_i/V_t > 1$.

4.7 Brugada algorithm

Brugada algorithm is the most widely known and commonly used algorithm (Figure 6) [50–64].

Brugada algorithm is as follows:

1. Is there concordance present in the precordial leads (leads V1-V6)?

“Are all of the QRS complexes completely upright, or downward in the precordial leads?”

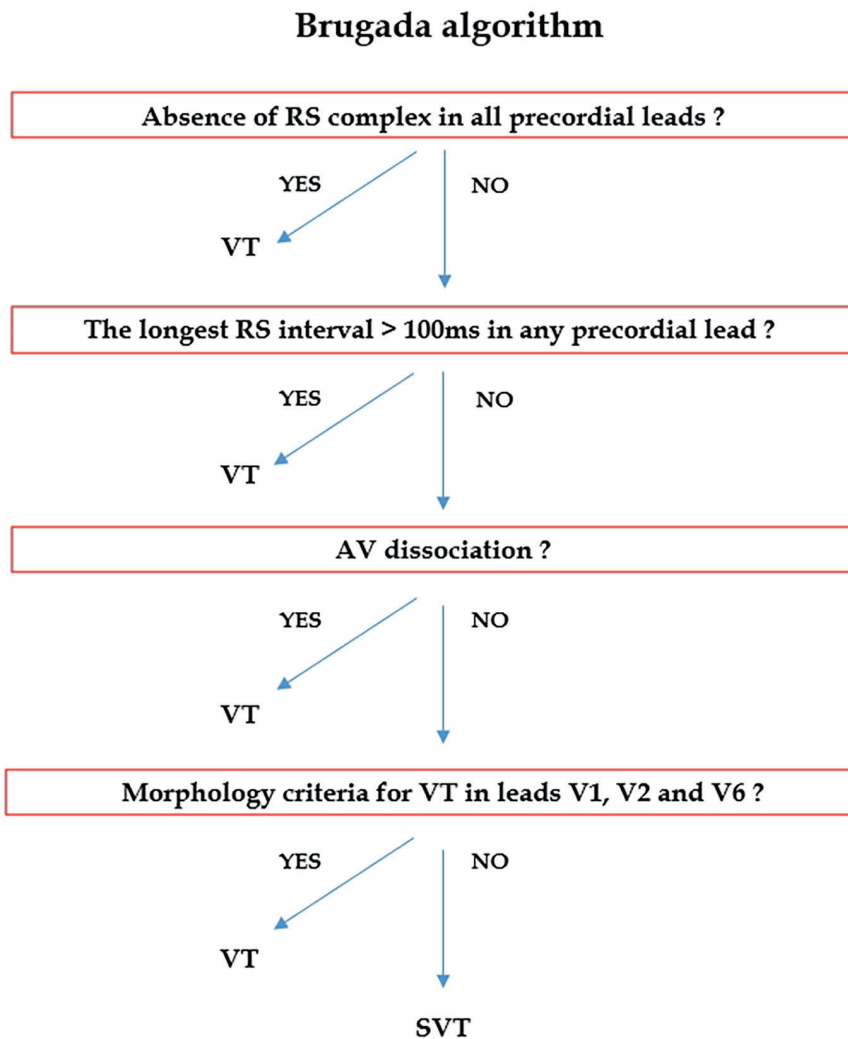


Figure 6.
Brugada algorithm.

Right bundle branch block morphology	Lead V1: Monophasic R, biphasic qR, broad R (>40 ms), Rsr' (the so-called 'rabbit ears' sign) Lead V6: R:Sratio < 1
Left bundle branch block morphology	Lead V1-2: Broad R wave, slurred or notched downstroke of S wave, delayed nadir of S wave Lead V6: Q or QR or QS wave

Table 4.
Morphology criteria for VT in leads V1, V2 and V6.

If the answer is yes, then VT is the diagnosis

2. Is the R to S interval (between the onset of the R wave and the nadir of the S wave) > 100 ms in any one precordial lead?

If the answer is present, then VT is the diagnosis

3. Is AV dissociation present?

“AV dissociation occurs when P waves are seen at different rates than the QRS complexes.”

If the answer is present, then VT is the diagnosis

4. Examine the morphology of the QRS complex to see if it meets the specific criteria for VT, as **Table 4**.

5. Conclusions


The ECG criteria or algorithms for the diagnosis of NCTs and WCTs has undergone evolution and development in concert with the field of cardiology itself, but the necessity of a correct diagnosis remains unchanged [50–64]. The world has not yet seen the ‘one criterion to end all criteria’ or ‘simplest criterion’ with high sensitivity and specificity, and it seems unlikely to appear in our near future. Therefore, physicians or cardiologists should be cautioned against overreliance in these ECG criteria or algorithms for the interpretation of the ECGs.

Author details

Bong Gun Song
Cardiac and Vascular Center, Seongnam Citizens Medical Center (SCMC),
Republic of Korea

*Address all correspondence to: aerok111@hanmail.net

IntechOpen

© 2022 The Author(s). Licensee IntechOpen. This chapter is distributed under the terms of the Creative Commons Attribution License (<http://creativecommons.org/licenses/by/3.0>), which permits unrestricted use, distribution, and reproduction in any medium, provided the original work is properly cited. 

References

- [1] Bellet S. Clinical disorders of the heart beat. 3rd ed. Philadelphia: Lea & Febiger; 1971
- [2] Hayes JJ, Stewart RB, Greene HL, et al. Narrow QRS ventricular tachycardia. *Annals of Internal Medicine*. 1991;**114**:460-463
- [3] Katritsis DG, Josephson ME. Differential diagnosis of regular, narrow-QRS tachycardias. *Heart Rhythm*. 2015;**12**:1667-1676
- [4] Brugada J, Katritsis D, Arbelo E, et al. 2019 ESC guidelines for the management of supraventricular tachycardias. The Task Force for the management of patients with supraventricular tachycardia of the European Society of Cardiology (ESC). *European Heart Journal*. 2019;**41**:655-720
- [5] Bar FW, Brugada P, Dassen WRM, et al. Differential diagnosis of tachycardia with narrow QRS complex (shorter than 0.12 second). *The American Journal of Cardiology*. 1984;**54**:555-560
- [6] Vereckei A, Duray G, Szénási G, et al. Application of a new algorithm in the differential diagnosis of wide QRS complex tachycardia. *European Heart Journal*. 2007;**28**:589-600
- [7] Brugada P, Brugada J, Mont L, et al. A new approach to the differential diagnosis of a regular tachycardia with a wide QRS complex. *Circulation*. 1991;**83**:1649-1659
- [8] Wellens HJJ. Ventricular tachycardia: diagnosis of broad QRS complex tachycardia. *Heart*. 2001;**86**:579-585
- [9] Wellens HJJ, Bar FW, Lie KL. The value of the electrocardiograms in the differential diagnosis of a tachycardia with a widened QRS complex. *The American Journal of Medicine*. 1978;**64**:27-33
- [10] Abedin Z. Differential diagnosis of wide QRS tachycardia: A review. *Journal of Arrhythmia*. 2021;**37**(5):1162-1172
- [11] Stewart RB, Bardy GH, Greene H. Wide complex tachycardia: Misdiagnosis and outcome after emergent therapy. *Annals of Internal Medicine*. 1986;**104**:766-771
- [12] O'Rourke SF, Sauvage A, Evans PA. Paroxysmal supraventricular tachycardia: improving diagnosis and management within the accident and emergency department. *Emergency Medicine Journal*. 2004;**21**:495-497
- [13] Bogun F, Anh D, Kalahasty G, et al. Misdiagnosis of atrial fibrillation and its clinical consequences. *The American Journal of Medicine*. 2004;**117**:636-642
- [14] Benditt DG, Pritchett EL, Smith WM, et al. Ventriculoatrial intervals: Diagnostic use in paroxysmal supraventricular tachycardia. *Annals of Internal Medicine*. 1979;**91**:161-166
- [15] Kotadia ID, Williams SE, O'Neill M. Supraventricular tachycardia: An overview of diagnosis and management. *Clinical Medicine (London, England)*. 2020;**20**(1):43-47
- [16] Kalbfleisch SJ, el-Atassi R, Calkins H, et al. Differentiation of paroxysmal narrow QRS complex tachycardias using the 12-lead electrocardiogram. *Journal of the American College of Cardiology*. 1993;**21**:85-89
- [17] Akhtar M. Supraventricular tachycardias. *Electrophysiologic*

mechanisms, diagnosis and pharmacologic therapy. In: Josephson ME, Wellens HJJ editors. *Tachycardias: Mechanisms, Diagnosis, Treatment*. Philadelphia: Lea & Febiger; 1984. p.137

[18] Josephson ME, Kastor JA. Supraventricular tachycardia: Mechanisms and management. *Annals of Internal Medicine*. 1977;**87**:346-358

[19] Ganz LI, Friedman PL. Supraventricular tachycardia. *The New England Journal of Medicine*. 1995;**332**:162-173

[20] Kesh Hebbar A, Hueston WJ. Management of common arrhythmias: part I Supraventricular arrhythmias. *American Family Physician*. 2002;**65**:2479-2486

[21] Obel OA, Camm AJ. Supraventricular tachycardia. ECG diagnosis and anatomy. *European Heart Journal*. 1997;**18**(Suppl. C):C2-C11

[22] Saoudi N, Cosìo F, Waldo A, et al. Working Group of Arrhythmias of the European of Cardiology and the North American Society of Pacing and Electrophysiology. A classification of atrial flutter and regular atrial tachycardia according to electrophysiological mechanisms and anatomical bases. A Statement from a Joint Expert Group from the Working Group of Arrhythmias of the European Society of Cardiology and the North American Society of Pacing and Electrophysiology. *European Heart Journal*. 2001;**22**:1162-1182

[23] Rosen MR, Fisch C, Hoffman BF, et al. Can accelerated atrioventricular junctional escape rhythms be explained by delayed afterdepolarizations? *The American Journal of Cardiology*. 1980;**45**:1272-1284

[24] Akhtar M, Jazayeri MR, Sra J, et al. Atrioventricular nodal reentry: Clinical, electrophysiological, and therapeutic considerations. *Circulation*. 1993;**88**:282-295

[25] Durrer D, Schoo L, Schuilenburg RM, et al. The role of premature beats in the initiation and the termination of supraventricular tachycardia in the Wolff-Parkinson-White syndrome. *Circulation*. 1967;**36**:644-662

[26] Coumel P, Attuel P. Reciprocating tachycardia in overt and latent preexcitation: influence of functional bundle branch block on the rate of the tachycardia. *European Journal of Cardiology*. 1974;**1**:423-436

[27] Kossaify A, Zeeny M. Electrocardiographic and electrophysiologic insights into atrioventricular nodal re-entry tachycardia: Diagnostic update. *Clinical Medicine Insights Cardiology*. 2012;**6**:111-117

[28] Kwaku KF, Josephson ME. Typical AVNRT--an update on mechanisms and therapy. *Card Electrophysiol Rev* 2002;**6**:414

[29] Letsas KP, Weber R, Siklody CH, et al. Electrocardiographic differentiation of common type atrioventricular nodal reentrant tachycardia from atrioventricular reciprocating tachycardia via a concealed accessory pathway. *Acta Cardiologica*. 2010;**65**:171-176

[30] Willems S, Shenasa M, Borggreffe M, et al. Atrioventricular nodal reentry tachycardia: Electrophysiologic comparisons in patients with and without 2:1 infra-His block. *Clinical Cardiology*. 1993;**16**:883-888

[31] Reddy GV, Schamrot L. The localization of by-pass tracts in the

- Wolff–Parkinson–White syndrome from the surface electrocardiogram. *American Heart Journal*. 1987;**113**:984-995
- [32] Kastor JA. Multifocal atrial tachycardia. *The New England Journal of Medicine*. 1990;**322**:1713-1717
- [33] Marriott HJL, Sandler IA. Criteria old and new for differentiating between ectopic ventricular beat and aberrant ventricular conduction in the presence of atrial fibrillation. *Progress in Cardiovascular Diseases*. 1966;**9**:18-28
- [34] Jolobe OMP. Caveats in preexcitation-related atrial fibrillation. *The American Journal of Emergency Medicine*. 2010;**28**:252-253
- [35] Campbell RWF, Smith RA, Gallagher JJ, et al. Atrial fibrillation in the preexcitation syndrome. *The American Journal of Cardiology*. 1977;**40**:514-520
- [36] Morady F, Sledge C, Shen E, et al. Electrophysiologic testing in the management of patients with the Wolff–Parkinson–White syndrome and atrial fibrillation. *The American Journal of Cardiology*. 1983;**51**:1623-1628
- [37] Yadav AV, Nazer B, Drew BJ, et al. Utility of conventional electrocardiographic criteria in patients with idiopathic ventricular tachycardia. *JACC Clinical Electrophysiology*. 2017;**3**:669-677
- [38] Steurer G, Gursoy S, Frey B, et al. The differential diagnosis on the electrocardiogram between ventricular tachycardia and preexcited tachycardia. *Clinical Cardiology*. 1994;**17**:306-308
- [39] Klein GJ, Bashore TM, Sellers TD, et al. Ventricular fibrillation in the Wolff–Parkinson–White syndrome. *The New England Journal of Medicine*. 1979;**301**:1080-1085
- [40] Klein GJ, Gulamhusein SS. Intermittent preexcitation in the Wolff–Parkinson–White syndrome. *The American Journal of Cardiology*. 1983;**52**:292-296
- [41] Littmann L, McCall MM. Ventricular tachycardia may masquerade as supraventricular tachycardia in patients with preexisting bundle-branch block. *Annals of Emergency Medicine*. 1995;**26**:98-101
- [42] Dancy M, Camm AJ, Ward D. Misdiagnosis of chronic recurrent ventricular tachycardia. *Lancet*. 1985;**2**:320-323
- [43] Garner JB, Miller JB. Wide complex tachycardia – ventricular tachycardia or not ventricular tachycardia. that remains the question. *Arrhythmia and Electrophysiology Review*. 2013;**2**(1):23-29
- [44] Wellens HJJ. Electrophysiology. Ventricular tachycardia: Diagnosis of broad complex tachycardia. *Heart*. 2001;**86**:579-585
- [45] Jastrzebski M, Kukla P, Czarnecka D, et al. Comparison of five electrocardiographic methods for differentiation of wide QRS-complex tachycardias. *Europace*. 2012;**14**:1165-1171
- [46] Katritsis DG, Brugada J. Differential diagnosis of wide QRS tachycardias. *Arrhythm Electrophysiol Rev*. 2020;**9**(3):155-160
- [47] Page RL, Joglar JA, Caldwell MA, et al. 2015 ACC/AHA/HRS guideline for the management of adult patients with supraventricular tachycardia: A report of the American College of Cardiology/ American Heart Association Task Force on Clinical Practice Guidelines and the Heart Rhythm Society. *Journal of the American College of Cardiology*. 2016;**67**:e27-e115

- [48] Vereckei A. Current algorithms for the diagnosis of wide QRS complex tachycardias. *Current Cardiology Reviews*. 2014;**10**(3):262-276
- [49] Alzand BSN, Crijns HJGM. Diagnostic criteria of broad QRS complex tachycardia: Decades of evolution. *Europace*. 2011;**13**:465-472
- [50] Jastrzebski M, Moskal P, Kukla P, et al. Specificity of wide QRS complex tachycardia criteria and algorithms in patients with ventricular preexcitation. *Annals of Noninvasive Electrocardiology*. 2018;**23**:e12493
- [51] Lau EW, Ng GA. Comparison of the performance of three diagnostic algorithms for regular broad complex tachycardia in practical application. *Pacing and Clinical Electrophysiology*. 2002;**25**:822-827
- [52] Jastrzebski M, Sasaki K, Kukla P, et al. The ventricular tachycardia score: A novel approach to electrocardiographic diagnosis of ventricular tachycardia. *Europace*. 2016;**18**:578-584
- [53] Brady WJ, Skiles J. Wide QRS complex tachycardia: ECG differential diagnosis. *The American Journal of Emergency Medicine*. 1999;**17**:376-381
- [54] Oreto G, Luzzo F, Satullo G, et al. Wide QRS complex tachycardia: An old and new problem. *Giornale Italiano di Cardiologia*. 2009;**10**:580-595
- [55] Roberts-Thomson KC, Lau DH, Sanders P. The diagnosis and management of ventricular arrhythmias. *Nature Reviews. Cardiology*. 2011;**8**:311-321
- [56] Gupta AK, Thakur RK. Wide QRS complex tachycardias. *The Medical Clinics of North America*. 2001;**85**:245-266
- [57] Barold SS, Stroobandt RX, Herweg B. Limitations of the negative concordance pattern in the diagnosis of broad QRS tachycardia. *Journal of Electrocardiology*. 2012;**45**:733-735
- [58] Volders PG, Timmermans C, Rodriguez LM, et al. Wide QRS complex tachycardia with negative precordial concordance: Always a ventricular origin? *Journal of Cardiovascular Electrophysiology*. 2003;**14**:109-111
- [59] Antunes E, Brugada J, Steurer G, et al. The differential diagnosis of a regular tachycardia with a wide QRS complex on the 12-lead ECG: Ventricular tachycardia. Supra-ventricular tachycardia with aberrant conduction and supraventricular tachycardia with anterograde conduction over an accessory pathway. *PACE*. 1994;**17**:1515-1524
- [60] Lau EW, Pathamanathan RK, NG GA et al. The Bayesian approach improves the electrocardiographic diagnosis of broad complex tachycardia. *Pacing and Clinical Electrophysiology*. 2000;**23**:1519-1526
- [61] Sternick EB, Timmermans C, Sosa E, et al. The electrocardiogram in sinus rhythm and during tachycardia in patients with anterograde conduction over Mahaim fibers: The role of the "rS" pattern in lead III. *Journal of the American College of Cardiology*. 2004;**44**:1626-1635
- [62] Grimm W, Menz V, Hoffmann J, et al. Value of old and new electrocardiographic criteria for differential diagnosis between ventricular tachycardia and supraventricular tachycardia with bundle branch block. *Zeitschrift für Kardiologie*. 1996;**85**:932-942
- [63] Alberca T, Almendral J, Sanz P, et al. Evaluation of the specificity of

morphological electrocardiographic criteria for the differential diagnosis of wide QRS complex tachycardia in patients with intraventricular conduction defects. *Circulation*. 1997;**96**:3527-3533

[64] Isenhour JL, Craig S, Gibbs M, et al. Wide-complex tachycardia: continued evaluation of diagnostic criteria. *Academic Emergency Medicine*. 2000;**7**:769-773

[65] Sandler IA, Marriott HJL. The differential morphology of anomalous ventricular complexes of RBBB-type in lead V1. Ventricular ectopy versus aberration. *Circulation*. 1965;**31**:551-556

[66] Griffith M, de Belder MA, Linker NJ, et al. Multivariate analysis to simplify the differential diagnosis of broad complex tachycardia. *British Heart Journal*. 1991;**66**:166-174

[67] Griffith M, de Belder MA, Linker NJ, et al. Difficulties in the use of electrocardiographic criteria for the differential diagnosis of left bundle branch block pattern tachycardia in patients with structurally normal heart. *European Heart Journal*. 1992;**13**:478-483

[68] Griffith MJ, Garratt CJ, Mounsey P. Ventricular tachycardia as default diagnosis in broad complex tachycardia. *Lancet*. 1994;**343**:386-388

[69] Kindwall KE, Brown J, Josephson ME. Electrocardiographic criteria for ventricular tachycardia in wide complex left bundle branch block morphology tachycardias. *The American Journal of Cardiology*. 1988;**61**:1279-1283

[70] Pava LF, Perafan P, Badiel M, et al. R-wave peak time at DII: A new criterion for differentiating between wide complex QRS tachycardias. *Heart Rhythm*. 2010;**7**:922-926

[71] Vereckei A, Duray G, Szénási G, et al. A new algorithm using only lead aVR for the differential diagnosis of wide QRS complex tachycardia. *Heart Rhythm*. 2008;**5**:89-98

Section 2

Clinical Use of ECG

Chapter 4

Electrocardiogram and Its Interpretation of Cardiac Diseases in Cattle

*N. Devadevi, P. Vijayalakshmi, K. Rajkumar
and A. Abiramy Prabavathy*

Abstract

Electrocardiogram is a non-invasive method and applied easily to determine the cardiac functions and its abnormalities in cattle. This chapter deals with the anatomy and position of the heart in the thoracic cavity in cattle. Describes the indications, precautions and requirements for ECG in cattle. Positioning of the animals and methods to be followed for ECG examination. Guidelines to be followed to read the ECG graph, normal waves and values of ECG and interpretation of ECG in different diseases conditions. ECG is an aid in the diagnosis of diseases like atrial enlargement, ventricular hypertrophy, anemia, mineral and electrolyte imbalance, myocardial infarction and classification of cardiac arrhythmias.

Keywords: ECG, cattle, cardiac disease, cardiac arrhythmias, ECG graph

1. Introduction

Electrocardiography is the simple non-invasive technique that records the changing electrical activity/potential difference in the heart by positive and negative electrodes. It is a valuable aid in assessing the heart rate, rhythm, chamber size, cardiac conduction system and cardiac functions. It is considered one of the more sensitive tool for diseases of the heart [1, 2]. ECG in ruminants is primarily used in the detection of cardiac arrhythmias, disturbances in conduction and electrolyte imbalances. This will help to determine the prognosis of cardiac disease and for therapeutic considerations [3]. Whereas mild enlargement of chambers cannot be detected in cattle due to deeply penetrating Purkinje fibers and the depolarization and repolarization occurring concurrently over multiple minor fronts [4]. Devadevi *et al.* [5] reported that electrocardiography is a useful aid in diagnosis of anemia in cattle affected with benign bovine theileriosis. Fetal electrocardiograms in dairy cattle were found to be useful in detection of multiple pregnancies [6]. ECG was successfully used in the detection of cardiac arrhythmias and conduction disturbances in buffaloes affected with traumatic reticuloperitonitis [7].

2. ECG examination in cattle

2.1 Anatomy and position of heart in the thoracic cavity of cattle

The bovine heart lies in the middle mediastinum between the 3rd to 5th intercostal space predominantly to the left side of the median plane with the base lying dorsally and the apex present ventrally, close to the sternum. The heart is rotated to the left side about its vertical axis such that the right auricle is present on the left side.

The heart consists of four chambers – two atria and two ventricles and has a base and an apex with the apex being formed solely by the left ventricle. The heart is surrounded by the fibrous and serous pericardium with a small amount of serous fluid present in the pericardial cavity. Each electrical discharge begins at the sinoatrial (SA) node present on the right atrium and the depolarization spreads through the atrial muscles to the atrioventricular (AV) node. The conduction passes from the atria to the ventricles through the bundle of His which divides into the left and right bundle branches supplying the left and right ventricles respectively. The left bundle branch is further divided into the anterior and posterior fascicles. The conduction is then passed through the Purkinje fibers to the myocardium [8].

2.2 Precautions and requirements

Cattle are docile in nature but they are excited and restless in a new environment. The cattle should be kept in a pleasant environment and be allowed to take rest. Animals should not be subjected to an ECG immediately after arrival because of the increase in the heart rate and respiration rate due to stress during transport. This will in turn give a wrong diagnosis. The animal is allowed to take rest for 15 minutes before performing the ECG examination. This will reduce the error in the ECG. Cattle should be kept in the trevis for ECG examination and calves should be kept on a wooden table, floor or nonconductive materials. Animals should not be leaning on the trevis as it will interfere with the ECG examination. A thick rubber sheet is placed over the trevis to prevent electrical noise produced by alternate currents when the animal comes in direct contact with the trevis [9].

2.3 Indications for ECG

ECG is the best method to read the different kinds of arrhythmias in cattle. If the heart rate exceeds 90 beats/minute, it is called as sinus tachycardia and if it is less than 50 beats/minute it is called as sinus bradycardia. ECG is an ideal additional tool to find out the electrolyte and mineral deficiency in cattle. These imbalances commonly occur during the first 3 months of production in animals suffering from milk fever, hypomagnesemia, post parturient hemoglobinuria and ketosis. Animals suffering from severe diarrhea may be deficient in certain minerals like sodium, potassium, chloride, iron and magnesium which may result in poor prognosis and should be replaced with ideal intravenous or oral electrolyte therapy. ECG is one of the methods to find out the enlargement of the atrium and ventricles. Although in cattle, mild enlargement of the heart is difficult to detect because of the deep penetration of the Purkinje fibers. ECG can be used to check the heart rate in cattle which may be cross verified with auscultation methods. The average of the last six R-R intervals of the trace is calculated to obtain the heart rate as the animals are more relaxed toward the end of the recording [10].

2.4 Positioning of the animals

The positioning of the animals is important to get an accurate ECG. The cattle should be kept in the standing position inside the trevis for an ECG examination. Animals affected with milk fever, diarrhea, lactic acidosis, Downer cow syndrome, etc. may be sternally or laterally recumbent. In such cases, animals may be subjected to the ECG examination in their current position.

2.5 Methods of ECG and ECG machine

Bipolar lead systems (Base apex I, II, III and X, Y and Z of the orthogonal system) and Unipolar leads (aVF, aVR, aVL and thoracic) have been described in animals. In large animals for the detection of cardiac arrhythmias base lead II and Y lead of the orthogonal system are most commonly used [9].

In cattle, ECG examinations method followed is base apex limb lead II. After adequate rest, the animal is kept in standing position in a trevis. ECG gel is applied on the lead attachment sites. Three sites are selected for application of the clips (**Figure 1**). Positive lead I is attached between the 3rd-5th intercostal space on the left side behind the elbow. Negative lead II is attached to the caudal 1/3rd of the jugular furrow and neutral lead III is attached away from the other two leads at the wither point [11].

The ECG machine is simply a voltmeter or galvanometer that records the changes in the electrical potentials occurring during each cardiac cycle. These changes are recorded on an ECG paper with a grid by a stylus. The stylus gets deflected according to the intensity of the electrical activity. The ECG machine is connected to a monitor and has an inbuilt printer. The results are obtained almost immediately. The clip used in ECG examinations is called an alligator clips. These clips have a pointed mouth with serrated ends for firm holding of the thick cattle skin. The serrated ends are very sharp and hence before usage it should be rasped or blunted to prevent injury to the animals. Before application of the alligator clips the sites should be cleaned with surgical spirit and adequate ECG gel should be applied for better contact.

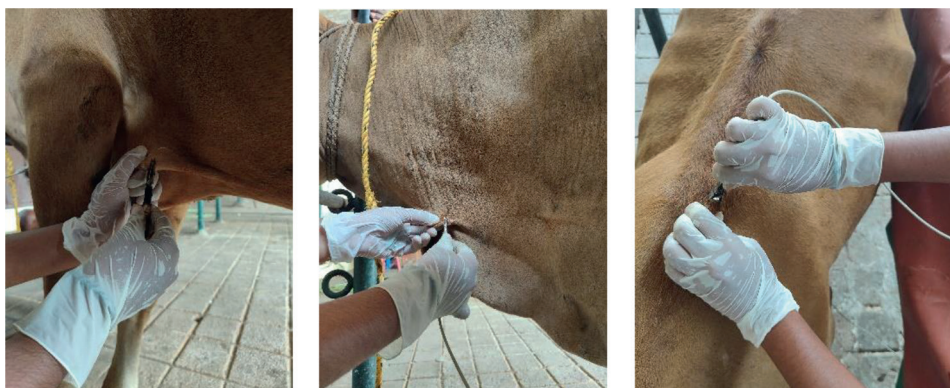


Figure 1. Positive lead I attached at the 3rd-5th intercostal space. Negative lead II attached at the caudal 1/3rd of the jugular furrow. Neutral lead III attached away from the first two leads at the point of withers.

2.6 Guidelines for reading the ECG

The ECG machine is equipped with a printer that generates a graphical representation on gridded paper of the electrical activity of the heart. The speed of the paper is set at 25 mm/second and the stylus present in the ECG records the deflection produced by the electrical impulses. The vertical axis of the grid denotes the voltage and direction of the deflection, either positive or negative, with respect to the baseline. The horizontal axis represents the time taken for each event in the cardiac cycle as well their sequence. The ECG paper is composed of a grid with small and large boxes. Each small box on the horizontal axis corresponds to a 0.04 second interval. Five small boxes form a large box which consequently represents 0.2 seconds. On the vertical axis, each small box corresponds to 0.1 mV.

2.7 ECG graph and its Normal waves

An ECG gives a graphical representation of the electrical changes occurring in the heart as a P-QRS-T complex. The electrical depolarization starting at the SA node travels across the atria creating a brief upward deflection of the stylus forming the P wave, representing atrial depolarization. The P-R interval is formed when the depolarization passes from the SA node to the AV node and into the ventricular tissue. The ventricular septum is the first to get depolarized in a direction away from the positive electrode creating a small negative deflection called the Q wave. A large positive/negative deflection, termed R wave, is created when the bulk of the ventricular myocardium gets depolarized. The S wave is formed when the remaining basilar portion of the ventricles gets depolarized. Thus the ORS complex is representative of ventricular depolarization. Complete ventricular depolarization is followed by repolarization before the next cardiac cycle. There is a difference in repolarization of the ventricular tissue creating a potential difference across the ventricular myocardium which forms the T wave.

The normal P wave amplitude and duration in Holstein cattle is 0.05–0.32 mV and 0.05–0.12 seconds respectively (**Figure 2**). In cattle, the QR and QS amplitudes are recorded separately and the normal values are 0.05–0.95 mV and 0.9–1.1 mV

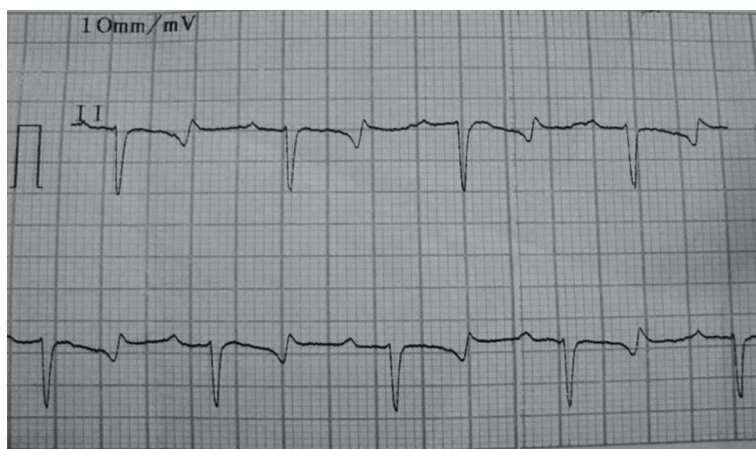


Figure 2.
Normal ECG pattern in cattle.

S.No	Parameters	Normal values
1	P wave amplitude (mV)	0.05–0.32
2	P wave duration (sec)	0.05–0.12
3	QR amplitude (mV)	0.05–0.95
4	QS amplitude (mV)	0.9–1.1
5	QRS duration (sec)	0.04–1.0
6	P-R duration (sec)	0.12–0.26
7	Q-T interval (sec)	0.22–0.48
8	T wave amplitude (mV)	0.05–0.8
9	T wave duration (sec)	0.05–0.16

Table 1.
 Normal ECG values in cattle.

respectively. The normal duration of the QRS complex is 0.04–1.0 seconds. The P-R interval and Q-T interval in normal Holstein cattle was found to be 0.12–0.26 seconds and 0.22–0.48 seconds respectively. In large animals, the T wave is more variable than in small animals and is generally not relevant in the detection of cardiac problems. The normal T wave amplitude and duration are 0.05–0.8 mV and 0.05–0.16 seconds respectively [10]. In **Table 1** the normal ECG values of cattle is given.

2.8 ECG graph and its interpretation

Variations in an ECG from the normal values of amplitude and duration in the P-QRS-T complex is indicative of cardiac dysfunction. In general, an increase in the amplitude of the P wave is suggestive of right atrial enlargement and increase in duration of the P wave is seen in left atrial enlargement (**Figure 3**). The QRS complex in bovines is negative and an increase in amplitude of QRS complex and duration of Q-T interval is characteristic of ventricular hypertrophy (**Figure 3**). A positive S wave is indicative of myocardial infarction. Variations in T was may be helpful in the

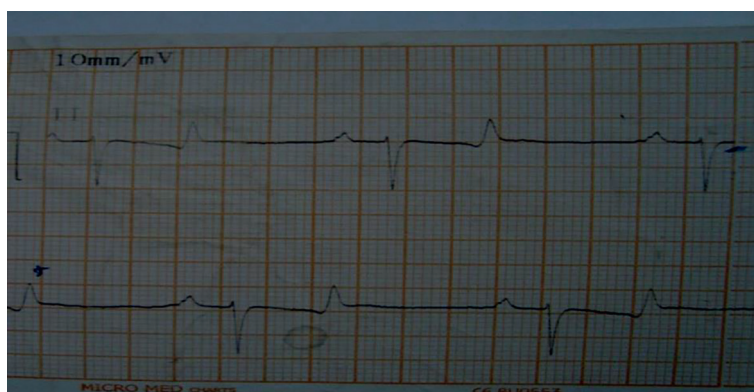


Figure 3.
 ECG shows notching of P wave indicative of atrial enlargement and increase in amplitude of QRS complex and QT interval indicative of ventricular enlargement in cattle.

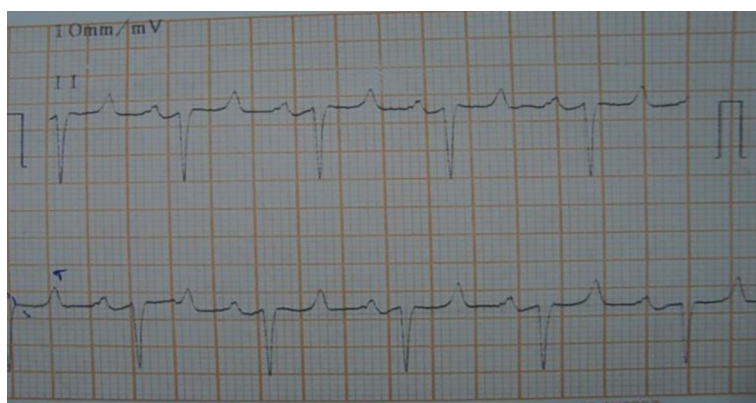


Figure 4.
ECG shows sinus tachycardia in cattle.

diagnosis of electrolyte and mineral imbalances. ECG alterations in some of the common cardiac diseases and electrolyte imbalances are described below.

Atrial fibrillation (AF) occurs due to focal ectopic firing arising from within the pulmonary veins and spreading to the atria [12]. AF is the most common cardiac arrhythmia present in milking cows. 50% of the cows with AF were previously diagnosed with ketosis suggestive of a relationship between the two conditions [13]. ECG recording of AF reveals absence/decreased amplitude of the P wave with a series of rapid and irregular waves (F wave) on the base line. The QRS complex is normal in amplitude and duration but irregular [12]. In cattle, the heart rate exceeds 90 beats/minute, it is called as sinus tachycardia (**Figure 4**) and if it is less than 47 beats/minute it is called as sinus bradycardia (**Figure 5**).

Endocarditis is an inflammatory disease affecting the layers of the endocardium in cattle due to bacterial infection. Bacterial endocarditis is most commonly of vegetative form (Healy, 1996). ECG examination in bovine vegetative endocarditis revealed deep QRS complex (1.7–2.5 mV) and tall T waves (0.8–1.5 mV) shown in the **Figure 6** [14].

Pericarditis is the inflammation of the pericardium with accumulation of serous or fibrinous inflammatory debris [15]. The most common cause of pericarditis in cattle is traumatic pericarditis [16] due to penetration of the pericardium by a hard foreign body. ECG taken in cattle affected with traumatic pericarditis shows decreased

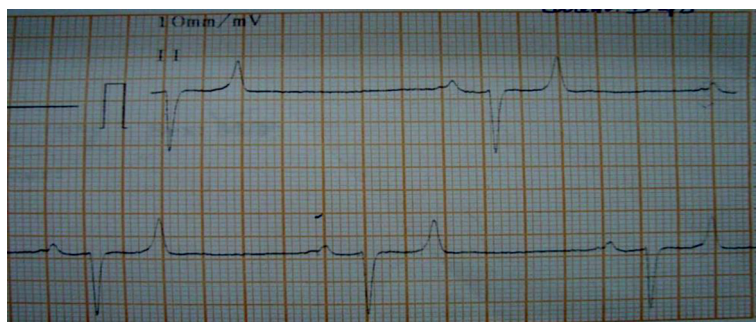


Figure 5.
ECG shows sinus bradycardia in cattle.

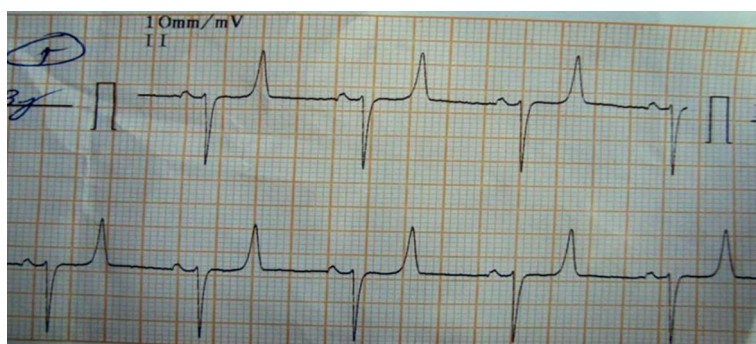


Figure 6.
ECG shows deep QRS complex and tall T wave in cattle with endocarditis.

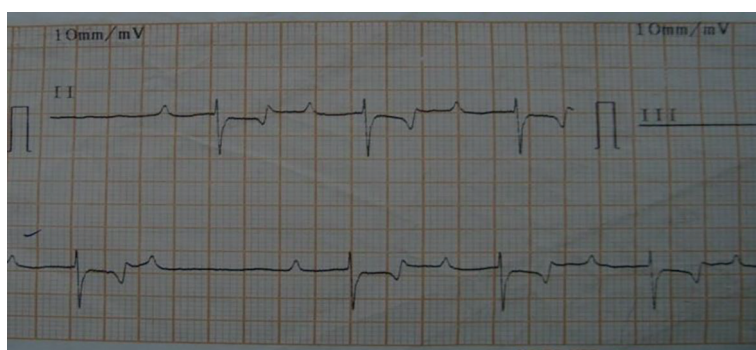


Figure 7.
ECG shows regular alteration in P, QRS or T wave and elevation of ST interval in cattle with pericarditis.

amplitude of QRS complex (<1.5 mV), regular alteration of P, QRS or T complexes and slurring/elevation in ST interval [17–19] shown in **Figure 7**.

In **Table 2**, ECG pattern of cattle with electrolyte and mineral imbalance was given. Hyperkalemia in an increase in potassium ion concentration in the blood caused by renal failure, severe dehydration and acidosis in calves with diarrhea [20]. The ECG in such animals shows wider QRS complex, tall T waves and deeper and higher S-T segment. A decrease in potassium ion concentration or hypokalemia occurs in case of inappetance, metabolic acidosis and increased excretion due to corticosteroid therapy combined with treatments used for ketosis [20]. The ECG recordings have tall and tent shaped T wave with an absence of P wave.

Hypocalcemia or parturient paresis is a condition common in periparturient cattle due to deficiency of calcium characterized by progressive neuromuscular degeneration, circulatory collapse and depressed consciousness [21]. Hypocalcemia is a common finding in case of Milk fever, Downer cow syndrome, Creeper cows, etc. The ECG is has a characteristic prolonged Q-T interval and lengthened S-T segment (**Figure 8**). Cows with hypocalcemia may have arrhythmias and sometimes complete heart block. Hypercalcemia is an increase in the levels of serum calcium most commonly due to primary hyperparathyroidism and malignancy [22, 23] as well as over supplementation of calcium in treatment of milk fever. Hypercalcemia decreases the atrial activity and increases ventricular activity [24]. ECG reveals short Q-T interval,

S. No	Condition	P wave	QRS complex	T wave	S wave	others
1	Hyperkalemia (Increased K ⁺)	*	Longer	Taller	Deeper Higher ST segment	Conduction Abnormalities
2	Hypokalemia (decreased K ⁺)	No P wave	*	Tall and Tent shape	*	Recorded in diarrhea calves
3	Hypercalcemia (Increased Ca ²⁺) / Hypothermia	*	Short QT interval	Widened / flattened	Short ST segment	Cause Acute Myocardial Infarction
4	Hypocalcemia (decreased Ca ²⁺)	*	Prolong QT interval	*	Lengthened ST segment	Recorded in Milk fever, Downers cow syndrome/ Creepers cow Arrhythmias and complete heart block
5	Hypomagnesemia (Decreased Mg ²⁺)	*	Short PQ interval and QRS complex Lesser degree shortening of QT	Negative	*	Causes Tachycardia, Arrhythmias and sudden death.
6	Severe Hypomagnesemia	*	*	High Peak	ST depression	Causes Sinus Tachycardia
7	HypoPhosphatemia (decreased P)	*	*	*	*	No change in ECG

Note: * indicate No change in waves.

Table 2.
ECG patterns in cattle with electrolyte and mineral imbalance.

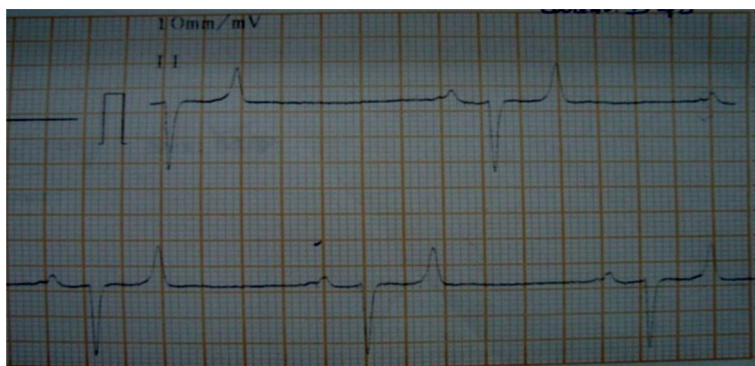


Figure 8.
ECG shows prolong QT interval and lengthened ST segment in cattle with hypocalcemia.



Figure 9.
ECG shows short PQ interval and QRS complex with negative T wave in cattle with hypomagnesemia.

flattened/widened T wave and short S-T segment. Hypercalcemia may cause acute myocardial infarction.

Hypomagnesemia tetany or grass tetany is caused by a deficiency of magnesium characterized by ataxia, recumbency, neuromuscular irritability, convulsions and tetanic spasms [25]. Cattle with hypomagnesemia (**Figure 9**) subjected to ECG shows short P-Q interval and QRS complex. The T wave is negative and there is a lesser degree of shortening of the Q-T interval.

3. Conclusions

Electrocardiography is currently the best method available for the detection of cardiac arrhythmias and conduction abnormalities [26]. Since Einthoven's invention of the first electrograph in 1895, there have been major advances in the study of cardiac diseases in both humans and animals. In cattle the base apex lead system is the most suitable for monitoring of cardiac function in cattle [9, 10]. Today, ECG is widely used in the field of veterinary medicine for the detection of cardiac arrhythmias and conduction abnormalities as well as to identify electrolyte and mineral imbalances which is valuable in the diagnosis of various disease conditions.

Acknowledgements

The technical assistance of Mr. Dias Nolan, veterinary student, is greatly appreciated. Thanks are extended to Ms. Carmel Prins, veterinary student, for typing the manuscript, to Dr. V. Vijayalakshmi, veterinary post-graduate student, for assisting in all the procedures involved in obtaining the required ECG readings. The authors extend their sincere gratitude to the Department of Veterinary Medicine and the Dean, Rajiv Gandhi Institute of Veterinary Education and Research, Puducherry.

Conflict of interest


The authors declare no conflict of interest.

Author details

N. Devadevi*, P. Vijayalakshmi, K. Rajkumar and A. Abiramy Prabavathy
Rajiv Gandhi Institute of Veterinary Education and Research, Puducherry, India

*Address all correspondence to: devivet_1983@yahoo.co.in;
devadevi.dr@gmail.com

IntechOpen

© 2022 The Author(s). Licensee IntechOpen. This chapter is distributed under the terms of the Creative Commons Attribution License (<http://creativecommons.org/licenses/by/3.0>), which permits unrestricted use, distribution, and reproduction in any medium, provided the original work is properly cited. 

References

- [1] Healy AM. Endocarditis in cattle-a review of 22 cases. *Irish Veterinary Journal*. 1996;**49**(1):4
- [2] Buczinski S, Fecteau G, DiFruscia R. Ventricular septal defects in cattle: A retrospective study of 25 cases. *The Canadian Veterinary Journal*. 2006;**47**(3):246
- [3] Radostits OM, Gay CC, Hinchcliff KW, Constable PD. *Veterinary Medicine, a Textbook of the Diseases of Cattle, Sheep, Goats, Pigs and Horses*. 10th ed. London, New York: Book power Saunders; 2010. pp. 1526-1531
- [4] Varshney JP. Electrocardiography in ruminants. *Electrocardiography. Veterinary Medicine*. 2020:245-259
- [5] Devadevi N, Rajkumar K, Vijayalakshmi P. Electocardiographic changes in cattle with bovine benign theileriosis. *Journal of Cell & Tissue Research*. 2018;**18**(2):6463-6465
- [6] Lindahl IL, Reynolds PJ, Allman KE. Fetal electrocardiograms in dairy cattle. *Journal of Animal Science*. 1968;**27**(5):1412
- [7] Sarita D, Varshney JP, Undirwade SC, Jadhav KM. Cardiac troponin-I and electrocardiographic findings in buffaloes with traumatic reticulo-pericarditis. *Ruminant Science*. 2014;**3**(2):177-180
- [8] Mansour M, Rowe J, Wilhite DR. In: *Guide to Ruminant Anatomy: Dissection and Clinical Aspects*. Hoboken: Wiley Blackwell; 2018. pp. 97-99
- [9] Areshkumar M, Abiramya A, Vijayalakshmi P, Selvi D. Analysis of base apex lead electrocardiographic technique in normal Jersey cross-bred dairy cows. *International Journal of Current Microbiology and Applied Sciences*. 2018;**7**(05):1772-1776
- [10] Rezakhani A, Paphan AA, Shekarfroush S. Analysis of base apex lead electrocardiograms of normal dairy cows. *Veterinářství*. 2004;**74**(5):351-358
- [11] Smith BP. In: Reef VB, Mcguirk SM, editors. *Large Animal Internal Medicine, Disease of the Cardiovascular System*. 5th ed. Rome: AGRIS; 2009. pp. 427-428
- [12] Staerk L, Sherer J, Ko D, Benjamin E, Helm R. Atrial Fibrillation. *Circulation Research*. 2017;**120**(9):1501-1517
- [13] Uchino T, Koyama H, Washizu M, Washizu T, Yamamoto T, Kobayashi K, et al. Atrial fibrillation in the cow, pig, dog, and cat. *Heart and Vessels. Supplement*. 1987;**2**:7-13
- [14] Mohamed T, Buczinski S. Clinicopathological findings and echocardiographic prediction of the localisation of bovine endocarditis. *Veterinary Record*. 2011;**169**(7):180
- [15] Grunder HD. Krankheitendes Herzens und des Herzbeutel. In: Dirksen G, Grunder HD, Stober M, editors. *InnereMedizinundChirurgie des Rindes*. 4th ed. Berlin, Germany: PareyBuchverlag. 2002. pp. 159-181
- [16] Roth L, King JM. Traumatic reticulitis in cattle: A review of 60 fatal cases. *Journal of Veterinary Diagnostic Investigation*. 1991;**3**(1):52-54
- [17] Reef VB, Gentile DG, Freeman DE. Successful treatment of pericarditis in a horse. *Journal of the American Veterinary Medical Association*. 1984;**185**(1):94-98

- [18] Foss RR. Effusive-constrictive pericarditis: Diagnosis and pathology. *Veterinary Medicine (USA)*. 1985;**80**:89-97
- [19] Freestone JF, Thomas WP, Carlson GP, Brumbaugh GW. Idiopathic effusive pericarditis with tamponade in the horse. *Equine Veterinary Journal*. 1987;**19**(1):38-42
- [20] Sweeney RW. Treatment of potassium balance disorders. *Veterinary Clinics of North America: Food Animal Practice*. 1999;**15**(3):609-617
- [21] Oetzel GK. Parturient paresis and hypocalcemia in ruminant livestock. *Veterinary Clinics of North America: Food Animal Practice*. 1988;**4**(2):351-364
- [22] Bilezikian JP. Primary hyperparathyroidism. *The Journal of Clinical Endocrinology & Metabolism*. 2018;**103**(11):3993-4004
- [23] Carrick AI, Costner HB. Rapid fire. *Emergency Medicine Clinics of North America*. 2018;**36**(3):549-555
- [24] Littledike ET, Glazier D, Cook HM. Electrocardiographic changes after induced hypercalcemia and hypocalcemia in cattle: Reversal of the induced arrhythmia with atropine. *American Journal of Veterinary Research*. 1976;**37**(4):383-388
- [25] Zelal A. Hypomagnesemia tetany in cattle. *Advances in Dairy Research*. 2017;**05**(02)
- [26] Fregin GF. Electrocardiography. *Veterinary Clinics of North America: Equine Practice*. 1985;**1**(2):419-432

Unshielded Magnetocardiography in Clinical Practice: Detection of Myocardial Damage in CAD Patients and in Patients Recovered from COVID-19

Illya Chaikovsky, Anatoly Kazmirchyk, Sergey Sofienko, You-Bin Liu, Ya-Feng Zhou, Xie Feng, Lin Xu and Yan-Fei Huang

Abstract

The chapter deals with magnetocardiography—a specific section of electrocardiography, which is designed to analyze the magnetic component of the electromagnetic field of the heart. Magnetocardiography is described as clinical information technology (IT), i.e., a set of methods, software, and hardware combined into a technological chain, the product of which is an automated diagnostic report. There are several examples of magnetocardiographic information technology implementation in clinical routine, aiming to register and evaluate subtle changes in the electromagnetic field of the heart for early diagnosis of the most common and dangerous heart diseases, especially coronary heart disease. It is shown that new metrics of analysis of spatial structure of 2D and 3D magnetocardiographic maps of current density distribution allow diagnosis with high accuracy of various forms of myocardial ischemia as well as myocardial damage in patients, recently recovered from COVID-19.

Keywords: magnetocardiography, coronary artery disease, non-coronarogenic diseases, myocardial damage, COVID-19, pattern recognition

1. Introduction

Effective diagnosis of heart disease remains one of the main tasks of clinical medicine due to the high prevalence and socio-economic importance of diseases such as cardiovascular diseases, which in recent decades, have become a pandemic [1]. In most European countries per 100,000 people. Population accounts for no more than 300 deaths from cardiovascular diseases. It is clear that the need to improve methods

for heart diseases detection is extremely actual. First of all, this applies to non-invasive methods that are the most accessible and safe.

Analysis of the electrical activity of the heart is still the most common, affordable, and cheapest method of objective examination of the heart. However, the sensitivity and specificity of routine electrocardiographic examination are not high enough. It is known, for example, that the resting ECG, assessed by its routine criteria, remains normal in approximately 50% of patients with chronic coronary heart disease, including during episodes of chest discomfort [2]. Improving diagnostics is possible only on the basis of innovative technologies.

The purpose of this chapter is to give an example of innovative technology introduced into practice, designed to register and evaluate subtle changes in the electromagnetic field of the heart for early diagnosis of the most common and dangerous heart diseases.

2. MCG definition and a brief insight to the magnetocardiography milestones

Magnetocardiography allows recording magnetic fields without body invasion and any risks through the skin-surface methodology. The detected fields are created by the heart's electrical activity. However, the signal is pretty weak to export the samples for storing and assessment, making the technique demanding, e.g., typical level of a magnetic field generated by heart muscle currents is between 10^{-10} and 10^{-12} Tesla, whereas the Earth's magnetic field and the urban noise levels are considerably higher (Figure 1).

The 1963 study by McFee and Balue records the first magnetocardiograms [3]. To obtain the game-changing magnetocardiogram human data they applied a couple of coils, containing a ferromagnetic core wrapped around with thin copper wire for

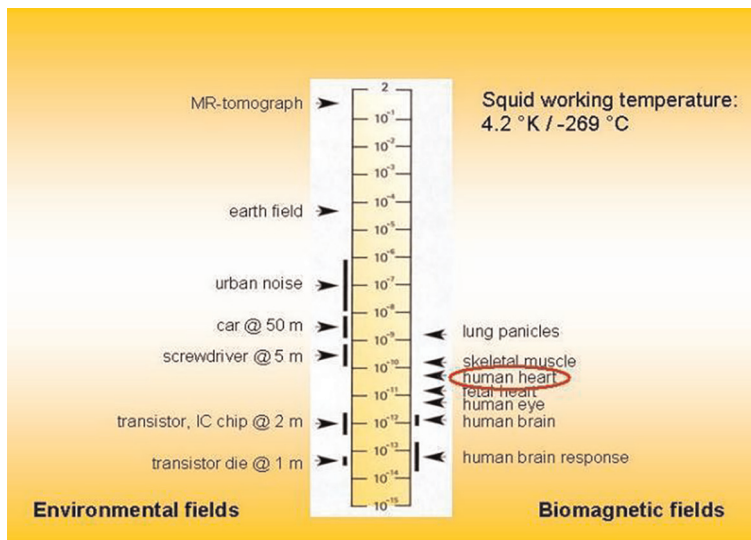


Figure 1. Specimens of generated magnetic fields.

several million times in each, kept at room temperature. The experiments were held at a far-away country location, to avoid the urban electromagnetic hindrance. Nevertheless, the output of the detector had flaws.

The research progress for alloys in the early 70's introduced the use of superconducting magnetometers. Cohen et al. initially applied the superconducting quantum interference device (SQUID) magnetometer in a room with antimagnetic protection, to detect a magnetocardiogram with improved dimensional accuracy and better spatial-to-noise property.

These SQUID magnetometers remain the only available device to record MCGs. The MCG studies by Cohen et al. had an enormous contribution to the basics of MCG recordings methodology, but cannot be considered a clinically relevant study, even though physicians took part in a few measurements. Then, in the early 80's Germany, USA, Finland, Japan, and Italy had some preliminary clinical research studies. At that time, a sole SQUID sensor was moved step by step across the measurement layout at the area near the anterior torso. The first commercially-made multi-channel systems became available in 1988–1990 with the help of Siemens, Philips, and BTI cooperation. In fact, only properly shielded rooms could be used for those systems' operation (**Figure 2**).

Today, there are numerous MCG laboratories in countries such as the United States, Germany, China, South Korea, Italy, Finland, Great Britain, Russia, Japan, Taiwan, India, and others.

In Ukraine, research in the field of magnetocardiography was initiated by specialists of the Institute of Cybernetics. VM Glushkov NASU together with specialists of the Institute of Cardiology in 1992. These studies began with the use of a single-channel MCG system. The work of the Kyiv group was pioneering from the very beginning because it was aimed at solving the most pressing problem—the diagnosis of coronary heart disease in difficult cases, i.e., in patients with uninformative results



Figure 2.
Philips multi-scan MCG system inside a highly-shielded room.



Figure 3.
9-channel MCG-system (Cardiomox) in unshielded hospital setting.

of routine tests such as ECG and resting echocardiography [4, 5]. Also, it is extremely important that the magnetocardiographic system developed by Ukrainian scientists can work in a normal unshielded room, which made the method of magnetocardiography suitable for wide clinical application (**Figure 3**).

3. Technical means of magnetocardiography and procedure of patients examination

Measurement of ultra-weak magnetic fields that occur during the work of the human heart and are almost a million times smaller than the magnitude of the Earth's magnetic field ($\approx 10^{-4} \text{Tl}$), requires very sensitive equipment. A significant increase in the sensitivity of biomagnetic measurements was achieved with the introduction of SQUID magnetometers, which operate on the basis of the stationary Josephson effect at a temperature of liquid helium (4.2 K). Beginning in 1970, when the SQUID magnetometer was first used [6], the MCG registration procedure became available for medical research and clinical practice.

Each of the currently known MCG systems can be divided into three functional modules. The first module (measuring) contains a registration part, which consists of sensors, antenna systems, and electronics for reading sensor signals. The second module (control) includes electronic units and microprocessor control of the entire system. The third (software module) provides computer processing of signals and their display using an application package with a high level of intelligent software. Additional hardware and software for protection against magnetic interference are used in each module.

Our MCG-system CARDIOMOXMCG 9 is installed in an unshielded clinical setting and during normal daytime operation, environmental noise was relatively constant. During acquisition, power lines represent the most dominant source of high amplitude noise (**Figure 4A**).

The position of the examined object is idle on the back. The MCG detections are held inside a six-by-six rectangular nettings that create an area (4 cm^2) over the precordial area making nine prethoracic sites. The sensor is moved to the thorax as

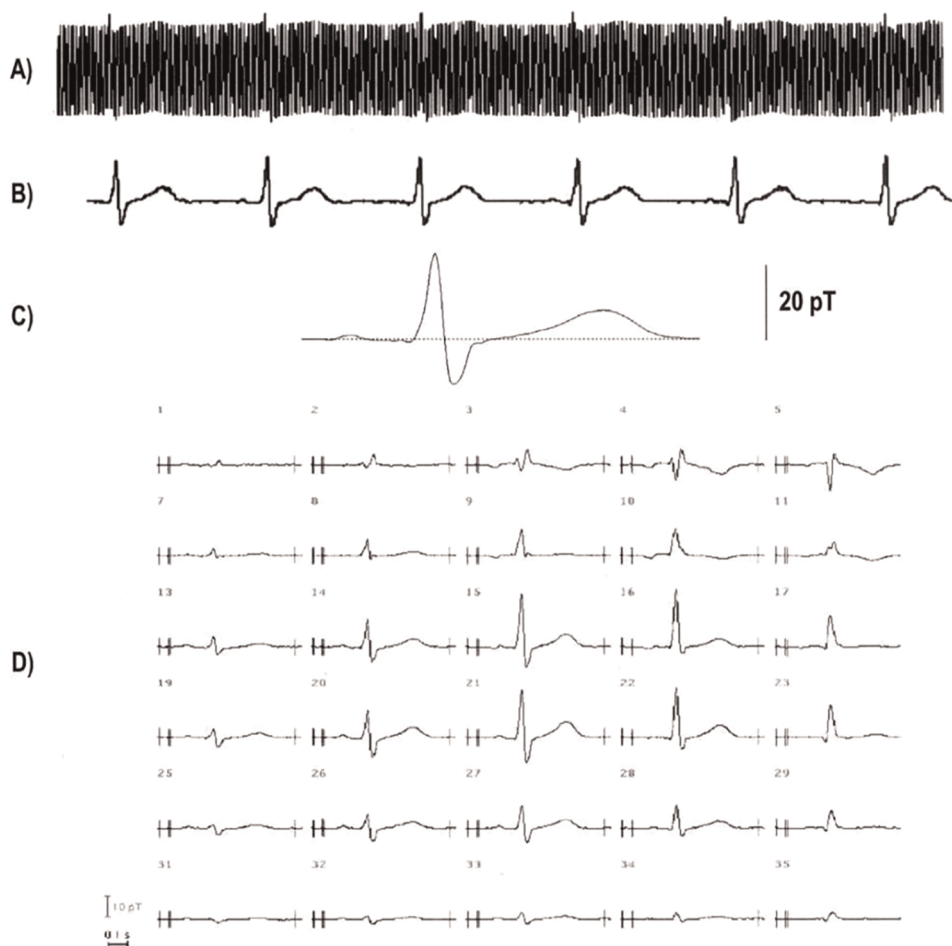


Figure 4. Samples of the MCG signals. (A) Initial channel 21 output (power noise included), (B) Same channel: 50 Hz notch filtered data, (C) Same channel: averaged signal, DC offset corrected prior to the P-wave, (D) Averaged signal in at all 36 registration sites.

close as possible, right above the heart, starting from the jugulum (**Figure 5**). All points are aligned with this reference point with the help of a rigid grid pitch.

Having the SQUID detector in an unmovable position over the adjustable table for examinations, the patient was moved to each designed grid position (9 in total) without leaving the idle lying state.

The above-described measuring grid is the most widely used. There are other types of grids, in some grids, each point is set taking into account its own anatomical landmark.

The registration records were taken to collect data from each site for 30 seconds with 1 kHz sampling frequency while a 0.1–120 bandpass filter was applied. At the same time, the surface ECG lead II was registered. All the obtained data was written onto memory devices for later processing. It took from 7 to 8 minutes to measure each intended location.

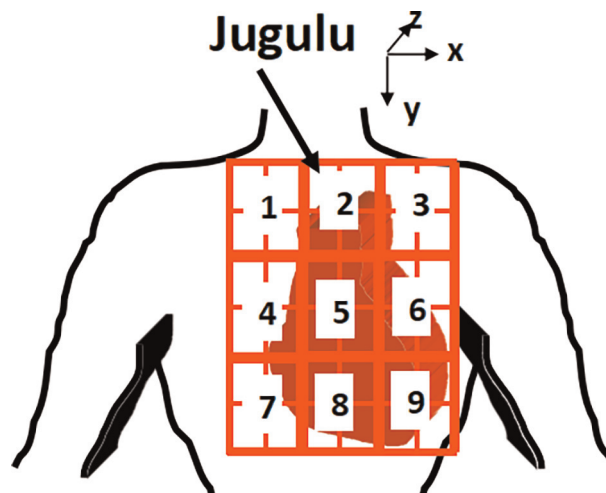


Figure 5.
A typical grid applied for getting the records, the precordial area covered has the dimensions 20 cm 20 cm. The starting point for the sensor is just higher the jugulum.*

4. The role of Electrophysiology for magnetocardiography

The ion current at cellular membranes in cardiac muscle cells defines their depolarisation and repolarisation. The latter also depends on single ions' temporally different permeability. Due to this, a shift arises in the membrane followed by changes in both the intra and extracellular volume currents. The spreading of these volume currents throughout the body causes the potential to alter the surface of the skin, so an electrocardiograph is able to detect the electrical potential changes once again. The nature and the functionality of the heart's specific cardiac conductivity system work in a way that it is electrically induced from the bottom state to the apex state. To apply the modeling for the heart's electrical activity, it can be substituted by a current dipole (also known as an equivalent dipole). Having the dipole with a distributed electrical field around it, the magnetic field should exist around it as well. The Biot-Savart approach helps to calculate the spatial dispersion induced by the dipole respectively. Here we define the magnetocardiogram as a recording of the frequent alternations in the magnetic field raising due to the cardiac cycle.

5. The MCG and the ECG key differences

Of course, MCG has similar morphological properties likewise ECG: we set a P-wave, a QRS complex, and T- and U- waves. Temporal correspondence between them is also most similar to ECG [7]. The majority of MCG devices make the magnetic field components measurement in a perpendicular way (radial or z-component) to the anterior chest (B_z). The key difference between dimensional layouts for ECG and MCG is their spatial alignment by 90° (**Figure 6**).

MCG is more sensitive to currents tangential to the chest surface, whereas ECG is more sensitive to radial currents.

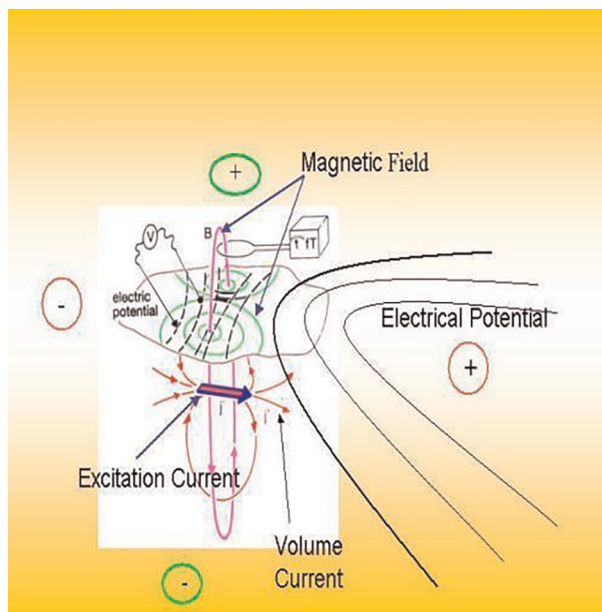


Figure 6.
Dimensional correspondence of electrical and magnetic fields.

Moreover, MCG is affected by isolated (vortex) current sources, which do not prevent any drops in potential on the body surface and thus the ECG is not able to detect them [8]. On the other hand, MCG is less influenced by conductivity alternations in the body (lungs, muscles, skin) than ECG. The MCG method does not invade the body at all, making the issues in the skin to electrode contact neglectable while being faced during the ECG. The switching in the ischemic diastolic TP and “true” ST switching is detected separately from each other by means of the direct-current MCG, due to the fact of missing potentials originating from the skin-electrode area.

6. Metrics and information technologies for the analysis of magnetocardiographic data based on two-dimensional visualization of the solution of the inverse problem of magnetostatics

The direct result of pre-processing of the data is 36 magnetocardiographic curves located at observation points—nodes of intersection of a rectangular grid, which is linked to the anatomical landmarks of the chest (Figure 7).

A detailed analysis of the morphology of MCG in healthy people was carried out. It was established that MCGs are similar to ECGs, recorded at the same points. The areas in which these or those elements of the MCG cardiac complex have the greatest amplitude have been analyzed. So, the wave P has the largest amplitude in the central zone of the upper half of the measuring grid corresponding to the V1 lead of ECG. The largest R—peak is recorded in the center of the measuring grid near the angle of the sternum, the deepest S-wave is in the left upper quadrant of the grid. The deepest q is recorded in the upper left corner of the grid. In this area, the ventricle complex has the form qRs or qR. The complex Rs prevails in the right part of the grid. The ST segment is located close to the isoline at all registration points. The highest positive tooth T is

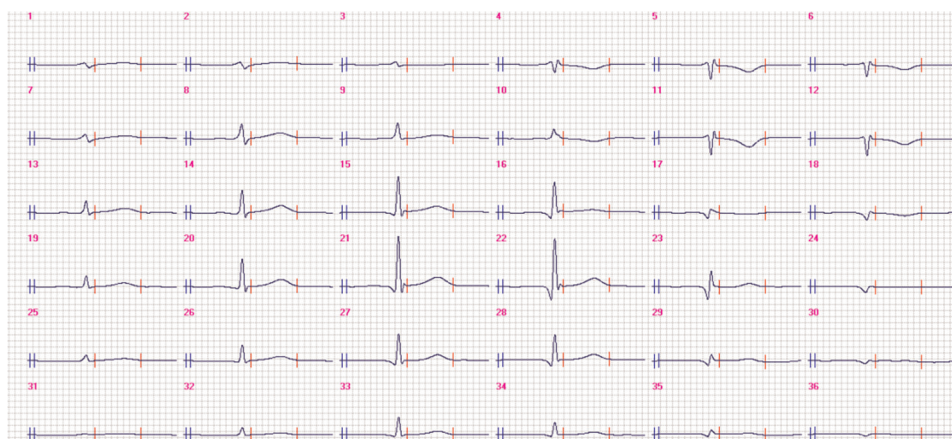


Figure 7.
36 MCG curves of healthy volunteer.

recorded in the same area as the largest R-peak, the deepest negative to this in the same area where the deepest S-wave is. The U-wave is always positive and best expressed in the left upper quadrant. The constitutional features of the normal MCG as well as features related to gender and age are also analyzed. It was found that men have significant differences in the magnitude of the QRS complex, depending on their age (up to 50 years the magnitude is higher), and growth (the higher growth, the greater the magnitude). In women, such differences are revealed in connection with weight—the more weight, the greater the magnitude. Totally for all categories, the coefficient of variation of the magnitude in healthy individuals is very high (0.48). This gives reason to doubt the advisability of applying criteria based on absolute values.

At the initial stage of development of magnetocardiography, the methods of its analysis copied the methods of analysis of electrocardiograms, the nomenclature of names of teeth, segments, and intervals developed for ECG analysis was used without changes. However, the analysis of individual MCG curves does not allow us to see the main advantage of magnetocardiography—high sensitivity to changes in the spatial distribution of the magnetic field at the points of the measurement plane and the associated density of ionic currents in the heart. This goal can be obtained after solving the inverse problem of magnetostatics.

This expression stands for the redesigning of the electrical activity in the heart using the recordings obtained above the surface of the human body. Since the measured magnetic field in MCG is found outside the very surface of the body and just over it, it is detected in a measurement surface from a short distance to the skin enclosing the chest cage.

Therefore, the next step in the analysis and interpretation of MCG data were methods closely related to the creation of modern information technologies.

For spatial fixation of data during MCG record the observation points are used. – These are nodes of intersection of a square grid. The magnetic signal is recorded at a frequency of 1 kHz. So the signal curve consists of individual “pieces” corresponding to individual “moments” of time. In other words, for each moment of time in 1 millisecond in points of a grid of measurements (6x6 points with a step of 40 mm on mutually perpendicular axes), it is possible to allocate simultaneously 36 values of a magnetic signal. If these signals are interpolated within the measurement area to a

more “frequent (with smaller distances between nodes)” grid, it is possible to construct a spatial distribution of the measured magnetic signal in the form of a magnetic field map. Thus, on the basis of 36 synchronous averaged MCG curves, two-dimensional (within 1 millisecond of time) magnetic field distribution maps are constructed using two-dimensional interpolation algorithms. Further, with the help of algorithms for solving the “inverse problem”, equiinduction maps of the magnetic field distribution can be “converted” into the corresponding instantaneous maps of the distribution of current density vectors (CDV maps). A fundamental novelty of the proposed analysis of MCG data is the use of a new methodological approach—to assess the dynamics of changes in current density during the cardio cycle using maps sequentially arranged in time (dynamic mapping). This approach has identified a number of new MCG indicators, which, on the one hand, have a clear electrophysiological meaning, and on the other—to exclude the impact on research results of technical and design features of the MCG system used due to the analysis of relative values.

In the next stage, the analysis of the dynamics of the selected parameters of CDV maps in the selected time intervals of the cardio cycle (QRS, ST-T, Ta-e) with an arbitrary or specified time step (4–10 ms).

CDV instant maps and sets of such maps during cardio cycle intervals are the main diagnostic image and object of analysis in magnetocardiography. Each individual map, and even more so a set of cards during a certain phase of the cardio cycle, contains multifaceted information. Therefore, to take full advantage of the method for analysis, it is necessary to use not a single indicator, but their combination.

The following concepts define the classification of the CDV maps.

The electrical generator while being repolarized can be considered as an extended current origin placed at the borderline zone splitting excited and unexcited areas of myocardium. Having normal ventricular repolarization, this wave-front of excitation which is also integrated into a homogeneous conductivity medium has to be moved left-downwards within a 10° – 80° sector. This model considers a couple of current types: the first one is known as “impressed current”, since it is originated from “impressed” currents which are the transmembrane potential gradient and passive volume currents. On the other hand, put into homogeneous conductivity these volume currents contribute to two vortices, which are symmetrical and equivalent. The processed mapping has a dipolar layout closer to ideal (**Figure 8**) containing only one location with relatively larger vectors pointing left and downwards.

Green arrows display the “impressed currents”, concentric-oriented curves represent current lines of the “volume” currents.

The appearance of inhomogeneity of conductivity due to some pathophysiological processes in the myocardium results in asymmetry and deformation of the vortexes (**Figure 9**), hence smaller portion of current vectors will be directed left-downwards.

Green arrows display the “impressed currents”, concentric-oriented curves represent current lines of the “volume” currents.

Following the greater raise in abnormality, likewise, for ischemia issues, we monitor the appearance of the supplementary excitation wavefronts. These wave-fronts are pathological and definitely will represent the layout of maps with a non-dipolar structure (**Figure 10**). Thus, we encounter so-called supplementary locations (clusters) of current vectors. Usually, their directions are not pointed left and downwards, leading to the state where the amount of normally pointed vectors continuously drops. However, we do not neglect situations where the areas with supplementary vectors are pointed left and downwards. Anyways, these kinds of layouts should be named

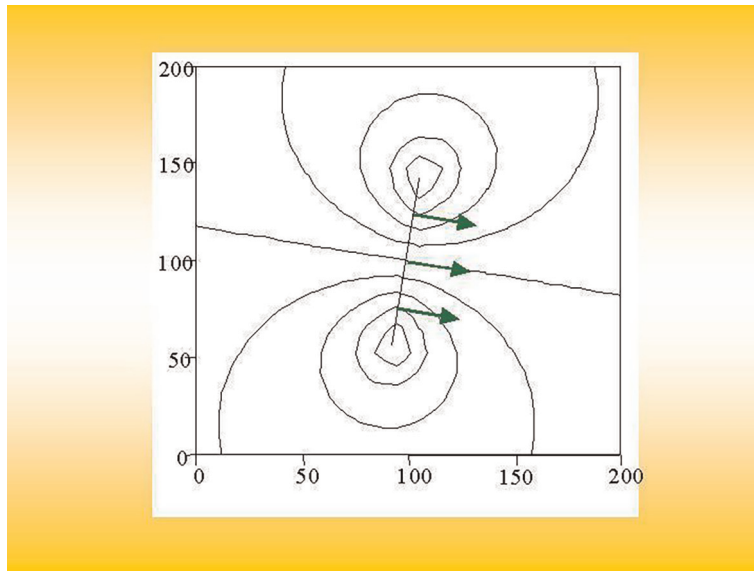


Figure 8.
The concept of current distribution in case of homogeneous conductivity.

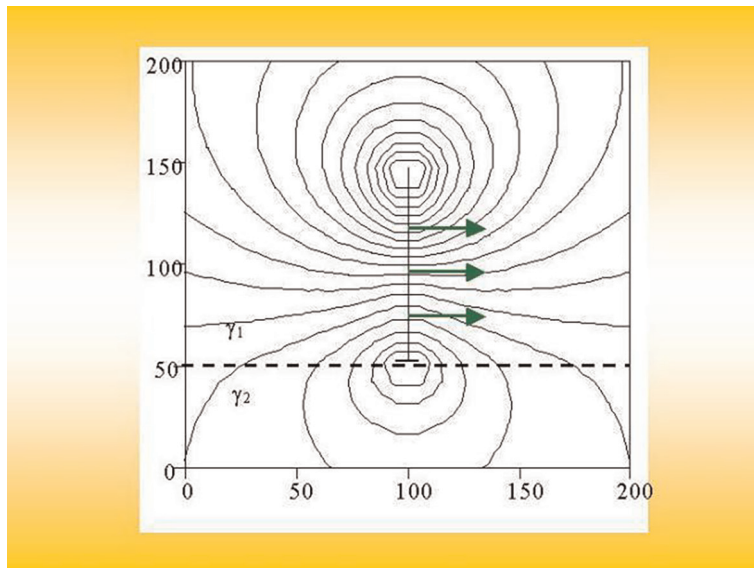


Figure 9.
Model of current distribution in the case of inhomogeneous conductivity (two zones with a ratio of conductivities $\epsilon_2/\epsilon_1=1/3$).

abnormal as well have given the decrease in homogeneity, i.e., the detection of supplementary areas (clusters).

Green arrows display the “impressed currents”, concentric-oriented ‘curves represent current lines of the “volume” currents.

Hence, the basic method of analysis of the spatial structure of the current distribution map is based on the concept of “proper” direction [9]. For each current

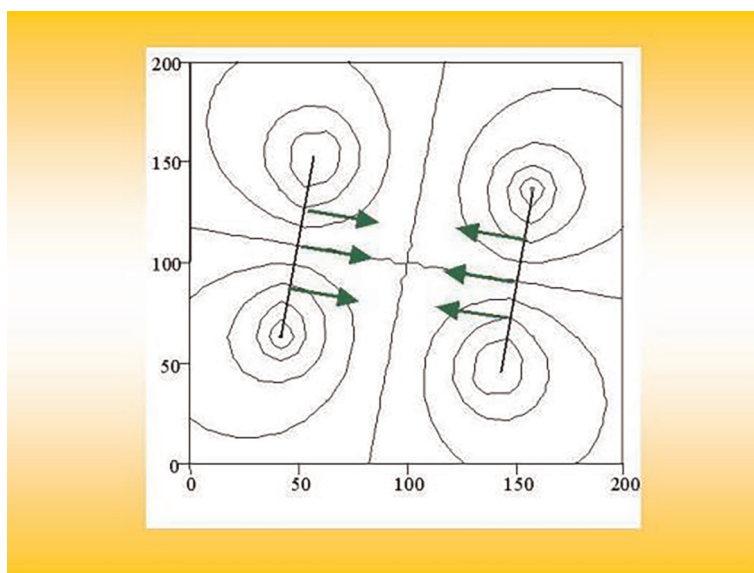


Figure 10.
The concept of current distribution with strong inhomogeneity (inhomogeneous conductivity (two excitation wave-fronts of equal strength)).

density vector, the normal direction is known, i.e., the sector within the pie chart from 0° to 180° and from -180° to 0° , which is used in the ECG, in which direction this vector is considered normal, i.e., “appropriate”. In this case, the “proper” direction has a clear link to the interval of the cardio cycle to which this map belongs. Thus, during ventricular repolarization (from point J to the end of the T wave) the direction in the sector of 10° – 80° is “appropriate”. It is known that during ventricular depolarization, the excitation sequentially covers the interventricular septum, anterior-apical area, sidewall, and posterior-inferior region of the left ventricle. Each of these phases of depolarization has its own “proper” direction of current density vectors (**Figure 11a–e**).

The quantitative parameter of this type of analysis is a normalized 100% anomaly index (Abnormality Index—AI), i.e., the ratio of the sum of the lengths of vectors directed in the correct, “proper” for each time directly to the sum of lengths of vectors having different from the “proper” direction. From the electrophysiological point of view, this indicator reflects the ratio of ion fluxes flowing in the “proper” direction and in a direction different from the “proper” one. The next stage of the analysis is the assessment of the processes of de- and repolarization of the ventricles in general. The average AI values during the QRS complex—AI_{QRS} total as well as during the ST-T interval—AI_{STT} total is calculated.

Another group of indicators is designed to assess the homogeneity of the repolarization process—the similarity of the spatial structure of the maps and the smoothness of the curve of the total current (i.e., the curve consisting of arithmetic sums of values of all current density vectors for each instantaneous map during the studied interval).

To quantify the homogeneity of the spatial structure of maps over time, the correlation coefficient (similarity) score between all maps during the ST-T interval was proposed. To estimate the smoothness of the curve of changes in the total current, the shape of this curve is analyzed. The duration (in% to the total duration of the ST-T

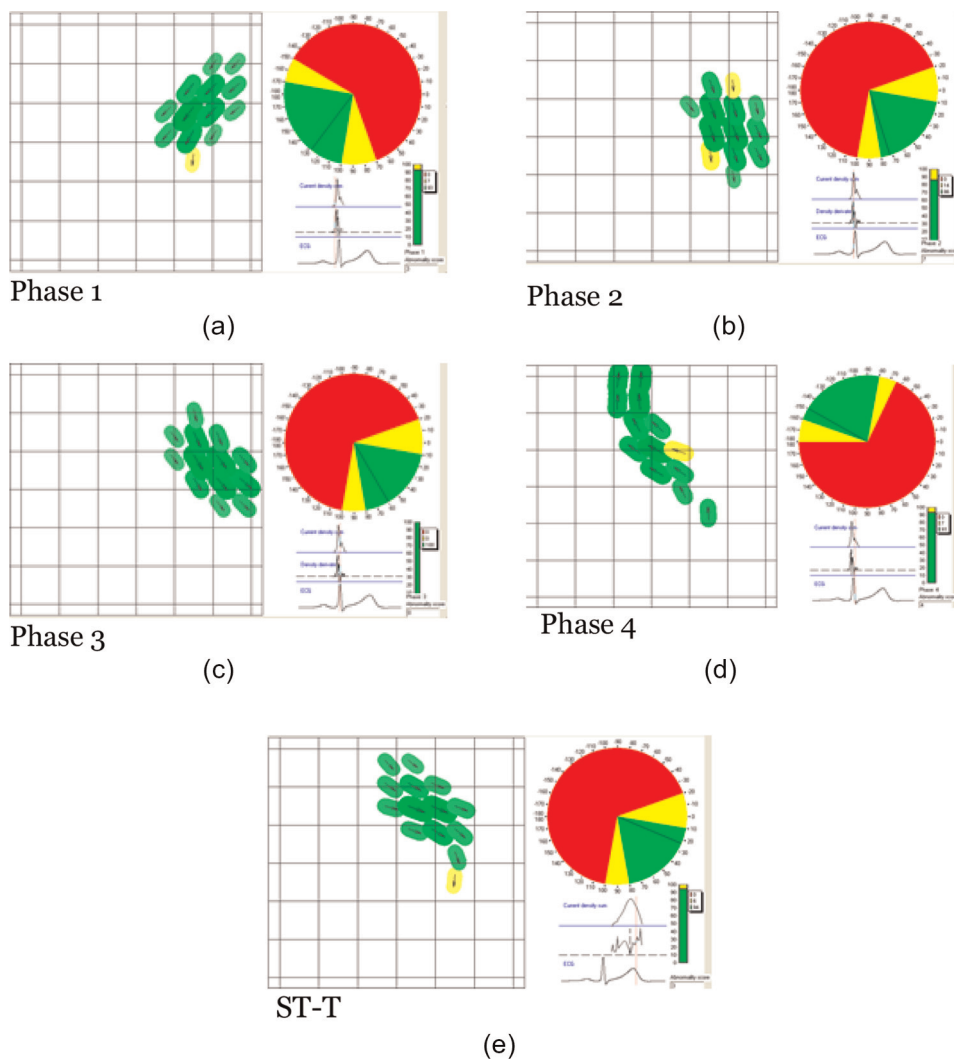


Figure 11. Distribution maps of CDV of a healthy volunteer (left) and pie charts (right) of depolarization: a) interventricular septum (phase 1), b) anterior wall and apex of the left ventricle (phase 2), c) lateral wall of the left ventricle (phase 3), d) basal myocardium (phase 4), e) ventricular repolarization (ST-T).

interval) of the section of this curve from its beginning to the inflection point, i.e., to the moment of the beginning of its monotonic growth (ADur) is determined. The higher the Scor value and the lower the Adur value, the more similar the CDV maps are within the ST-T interval and the higher the homogeneity of the repolarization process as a whole. Decreases in similarity score values and increases in Adur almost always occur due to the changes at the initial part of the ST segment. The duration of one initial site corresponds to the time during which some areas of the myocardium are in a later phase of the transmembrane action potential compared to neighboring areas. In other words, the duration of this section reflects the degree of regional heterogeneity of repolarization.

Finally, the time dependence curve of the correlation coefficient of the current map with the map at the apex of the R wave during the ORS complex is investigated.

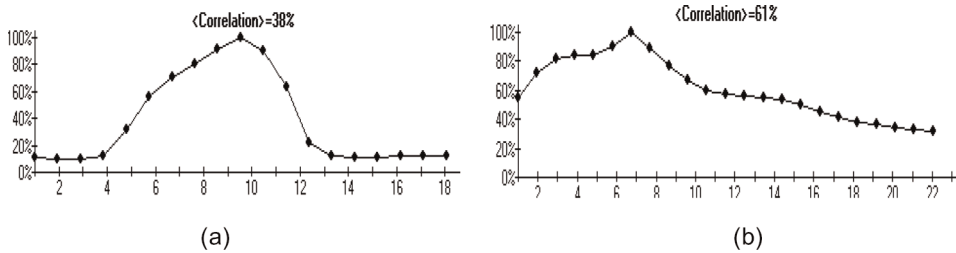


Figure 12. Influence curves of the correlation coefficient of the current map with a map on the top of the tooth R: in healthy volunteer; b) in patients with a large MI.

In other words, the degree of similarity of each current map with the map at the top of the tooth R, i.e., with the map in which the value of the total current is greatest. The correlation coefficient between all maps during the QRS—CcorQRS complex is calculated. The shape of the correlation curve of the current map with the map at the top of the R wave is also analyzed. Normally, this curve has 3 characteristic inflection points (**Figure 12a**)—between the first phases of depolarization, the 2nd and 3rd phases, and 3th and 4th phases. In pathology, these points, especially 1 and 3 are smoothed or completely absent (**Figure 12b**).

The calculation of the above set of temporal and spatial features is based on a key electrophysiological concept—the increase of electrical heterogeneity (heterogeneity) of the myocardium in the occurrence of pathological processes, such as ischemia.

In our opinion, one of the main ways to increase the functional efficiency of magnetocardiography is to build systems for automatic classification of magnetocardiograms based on the ideas and methods of machine learning and pattern recognition.

We have developed a method for analyzing CDV maps during ST-T intervals based on pattern recognition.

Correlation analysis was used to classify each current density map. The main idea of the method of current density distribution map classification based on correlation analysis is to find and compare the correlation coefficients of the map under analysis with each of the maps in the reference set. Reference sets consist of pre-classified by the doctor current density distribution maps, each of which belongs to one of the groups corresponding to a certain state of the cardiovascular system. For each of the classified maps, the correlation coefficients of the vector of values and the vector of directions with the corresponding vectors of each of the maps from the reference set are calculated as follows [10]:

$$\begin{aligned}
 r &= \frac{\sum_{i=1}^n (x_i - \bar{x})(y_i - \bar{y})}{\sqrt{\sum_{i=1}^n (x_i - \bar{x})^2 \sum_{i=1}^n (y_i - \bar{y})^2}} \\
 &= \frac{\sum_{i=1}^n (x_i - \bar{x})(y_i - \bar{y})}{\sqrt{\sum_{i=1}^n (x_i - \bar{x})^2 \sum_{i=1}^n (y_i - \bar{y})^2}}
 \end{aligned} \quad (1)$$

Where n is the dimension of the vectors, for our case $n = 100$, x_i , and y_i are values of vectors for which the correlation coefficient is calculated and \bar{x} and \bar{y} are the mean values of the vectors, calculated as follows:

$$\bar{x} = \frac{1}{n} \sum_{i=1}^n x_i \quad \bar{y} = \frac{1}{n} \sum_{i=1}^n y_i \quad (2)$$

$$y^- = 1n \sum i = 1nyi(3)y^- = 1n \sum i = 1nyi \quad (3)$$

After that, the values of the obtained correlation coefficients for two vectors are multiplied; thus, the resulting correlation coefficient is obtained, which takes into account both the modulus correlation and the direction of the current density vectors. As a result, a set of the resulting correlation coefficients with the maps of each group of the reference set is obtained for each map. After that, an array of m maximum values of the resulting correlation coefficient is formed for each group, and their average value is found. Thus, for each CDDM we obtain a set of key-value pairs with the groups corresponding to the state of the cardiovascular system as keys, and the above described average values of the maximum correlation coefficients as corresponding values. The maximum of these values indicates the group to which the map of the distribution of the current density to be classified should be assigned. The best result was obtained for m in the range of 1–5, and the accuracy of classification in these cases is highest and does not significantly depend on the number of maximum values; therefore, in this study, we use $m = 3$.

One of the methods for pattern classification is the k-nearest neighbor (k-NN) rule. It classifies each unlabeled object according to the majority label of its k-nearest neighbors in the training set. Despite its simplicity, the k-NN rule often yields competitive results and in certain domains, when cleverly combined with prior knowledge, it can help to solve even quite difficult classification tasks.

The result of k-NN classification depends significantly on the metric used to compute distances among different feature vectors. In [11], it was shown that using different distances for k-NN classification gives an opportunity to decrease the error rates for different classification problems, such as face recognition, spoken letter recognition, and text categorization. It was also demonstrated that a k-NN classifier with a correctly chosen distance metric shows better results, even when compared to SVM used for same classification tasks.

In this study, the three most commonly used metrics, which are special cases of Minkowski distance, Euclidian, Cityblock, and Chebychev, were examined. Let us consider X as a 1×32 feature vector of a classified CDDM and Y as a feature vector of each CDDM in the training set. In our study, binary classifiers with three different distance metrics were developed. A classifier with an Euclidian metric distance between two points X_s and Y_t , whose coordinates are values of X and Y , respectively, is defined as follows:

$$dst = (x_s - y_t)(x_s - y_t)'(4)dst = (x_s - y_t)(x_s - y_t) \quad (4)$$

For Cityblock (also known as Manhattan) metric:

$$dst = \sum_j = 1n x_{sj} - y_{tj}(5)dst = \sum_j = 1n |x_{sj} - y_{tj}| \quad (5)$$

where n is the size of vectors X and Y , and in our case $n = 32$ —number of features. For Chebychev metric:

$$dst = \{x_{sj} - y_{tj}\} \quad (6)$$

2142 current density distribution maps were analyzed, which were assigned to 6 different groups depending on the verified diagnosis of the patient. These maps amounted to 6 basic databases of reference images. Each of these databases includes maps that are most specific to a particular disease.

Group	1	2	3	4	5	6	7	8	9	10	11	12	13	14	15	16	17	18	19	Mean1	Mean2
Athler's heart	10.3	8.5	4.59	4.49	3.19	3.27	8.04	10.16	15.21	19.54	26.47	37.67	39.56	37.28	37.48	33.9	33.6	28.94	24.68	26.1	0
Norm	6.93	7.16	6.28	5.99	5	3.82	6.44	6.35	12.71	17.52	26.68	35.07	43.81	45.41	43.83	43.04	43.32	40.83	40.18	23.18	22.81
LVH 1	3.22	2.15	1	0.75	0.78	1.39	6.59	5.9	5.94	6.77	9.63	13.75	18.12	16.03	16.68	19.36	19.98	25.08	21.35	10.24	0
LVH 2	1.67	2.23	3.28	2.72	2.98	2.35	5.89	5.39	6.75	8.06	11.95	15.53	20.23	19.96	19.49	18.68	19.17	22.66	20.74	11.04	0
LVH 3	5.64	5.54	4.49	3.03	2.01	2.24	8.12	8.94	11.17	12.63	13.05	12.74	12.95	10.26	10.6	9.45	9	9.55	7.85	8.38	0
Non-coronariogenic diseases	7.85	8.71	9.67	8.94	8.98	8.21	11.59	12.83	17.21	20.82	28.01	35.18	36.62	42.53	43.17	40.95	41.26	33.61	38.56	23.93	0
Microvascular disease(M)	15.19	12.9	15.08	13.47	13.99	10	10.52	13.51	16.27	19.6	23.09	25.46	27.01	26.2	24.3	21.91	21.93	18.41	17.24	18.22	3.9
Myocardial damage	3.29	5.93	4.16	3.17	2.44	3.11	6.25	3.17	1.73	2.26	3.67	6.65	10.22	19.7	19.63	19.35	19.86	12.26	9.67	6.36	0
CAD 1	14.45	21.56	32.26	33.32	37.86	34.46	36.52	37.33	38.3	39.23	41.63	42.85	42.48	44.74	45.47	43.6	44.2	40.26	43.3	37.57	73.29
CAD 2	4.33	5.34	4.19	4.34	3.36	6.51	7.7	7.87	6.78	9.92	4.78	4.51	4.67	5.14	5.42	5.5	5.8	5.62	5.11	5.42	0
CAD 3	7.39	10.47	10.53	9.91	9.59	10.83	11.21	11.52	9.18	8.49	2.89	3.82	5.19	7.14	6.83	8.14	8.19	7.86	10.21	8.39	0
CAD 4	6.54	3.37	2.38	1.99	1.32	2.5	4.04	3.83	4.27	3.86	6	8.61	11.63	12.23	13.29	13.33	13.44	13.19	12.47	7.28	0
CAD 5	3.88	7.61	8.06	5.96	5.95	2.29	5.33	4.05	3.48	2.05	1.57	1.17	1.14	1.46	1.63	1.82	1.85	2.24	2.94	3.37	0

Figure 13. Correlation coefficients for the consecutive CDV maps relative to the reference base of maps for each of the 14 categories.

These groups are as follows: normal, left ventricular hypertrophy (LVH), non-coronary heart disease, microvascular disease, myocardial infarction, and coronary heart disease (coronary heart disease) other than MI. In turn, the norm group is divided into 2 subgroups, the LVH group—into 3 subgroups, and the coronary heart disease group—into 6 subgroups. Thus, in the end, we have 14 categories. Correlation coefficients were calculated for the current map relative to the reference base of maps for each of the 14 subcategories.

Next, the results of the classification of individual consecutive maps on the ST-T interval were averaged for the entire ST-T interval. As a result, we obtain the probabilities of belonging to a particular magnetocardiographic examination in each of the 14 categories for each MCG examination (**Figure 13**).

In this case, the highest probability of belonging to the category of coronary heart disease, subcategory 1

7. Clinical approbation of metrics of analysis of magnetocardiographic data on the basis of two-dimensional visualization of the solution of the inverse problem of magnetostatics. Multicenter studies

The purpose of using any diagnostic parameter is to formulate a clinically significant diagnostic conclusion, i.e.:

- decision on the presence or absence of a pathological process;
- in the case of a process—determining the severity.

The set of features has higher diagnostic accuracy than a single feature. Thus, there is a problem with forming from a set of parameters of a single complex indicator, which synthesizes various aspects of the information contained in each individual indicator. Such an indicator can be created on the basis of the method of linear discriminant analysis (LDA). As a result, a discriminant function is automatically built. If the value of the function is greater than the threshold, the results of the MCG test are positive, if less—negative.

Another, empirical-statistical approach, which is used to form a comprehensive index, is calculated on the basis of scores. When using this approach, the values of all quantitative indicators are a priori divided into ranges. When the value of an individual indicator falls into the appropriate range, it is given a certain number of points.

Then the number of points of all indicators is summed. If the sum of points exceeds a certain threshold, the MCG test is considered positive, if on the contrary—negative. If the test is positive, the number of points determines the severity of the pathology on the principle—the higher the score, the more pronounced the pathology. Such scores are widely used in electrocardiography (Sylvester score, Freuleher score, CIIS and others), as well as to assess the results of the test with dosed exercise (Duke's index). We have created an integrated scoring criterion of the additive type for the diagnosis of myocardial ischemia using MCG. The value of this criterion was recently investigated by us in two multicenter studies involving foreign colleagues. A two-center study was conducted at the National Military Medical Clinical Center and at the Catholic Clinical Philipppusstift (Essen, Germany) [12]. We examined 79 patients with complaints of chest pain and normal or non-informative results of ECG and echocardiography at rest, i.e., in difficult-to-diagnose cases. All patients underwent coronary ventriculography. According to the results of coronary angiography, patients were divided into subgroups with stenosis > 70% in at least one of the main coronary arteries (subgroup 1a) and a subgroup of persons without hemodynamically significant stenosis (subgroup 1b). Control group 2 consisted of 30 healthy volunteers close in age. **Table 1** shows the indicators of diagnostic value of the complex MCG index to detect significant stenosis of the coronary arteries in difficult-to-diagnose cases.

The goal of any diagnostic test is to reduce the uncertainty level and to increase the confidence of the investigator in valuable decision-making. The present study investigates a group of patients for whom this decision is performed on the basis of coronary angiography. The pretest probability of hemodynamically significant coronary artery stenosis in patients analyzed was about 50%; therefore, the degree of uncertainty is the highest in this case. Post-MCG probability to use analogous to post-ECG probability that a hemodynamically significant stenosis is absent is 85% in the case of negative result of MCG-study. In the case of a positive MCG result, the probability of haemodynamically significant stenosis is 93%.

Thus, the results of our MCG-study reduce uncertainty in decision-making. Coronary angiography should be considered for patients with positive MCG-results. In the case of negative MCG-results, the invasive procedure could be avoided.

An even larger multi-center study was conducted in three leading clinics in Beijing under the guidance of specialists from the main hospital of the Chinese Navy. A total of 133 people were examined (mean age 59 ± 3.1 years). All surveyed individuals were divided into three groups. The first group (61 people) consisted of patients with severe myocardial ischemia who met the criteria for revascularization: the degree of coronary artery stenosis was $\geq 80\%$ or was between 50% and 80%, with a margin of coronary blood flow ≤ 0.8 .

Diagnostic value parameters	Comparison of subgroups 1a и 1b	Comparison of subgroup 1a with subgroup 2
Sensitivity, %	93	93
Specificity, %	84	94
PPV, %	85	94
NPV, %	93	93

Table 1.
Diagnostic value of complex MCG index.

The second group (13 people)—patients whose myocardial ischemia is confirmed by the “gold standard”—invasive coronary angiography but has not yet met the criteria for revascularization. The third group (59 people) is the control group. The percentage of coincidence of ICG results and coronary angiography in each group was as follows: for severe coronary heart disease—85.45%, for mild coronary heart disease—77.78%, in the control group—87.10%.

Achieved a total sensitivity of 93.75%, a specificity of 87.10%, PPS was 88.24%, and NPV 93.10%.

Thus, magnetocardiographic examination is a reliable method of diagnosing chronic coronary heart disease, including in difficult-to-diagnose cases.

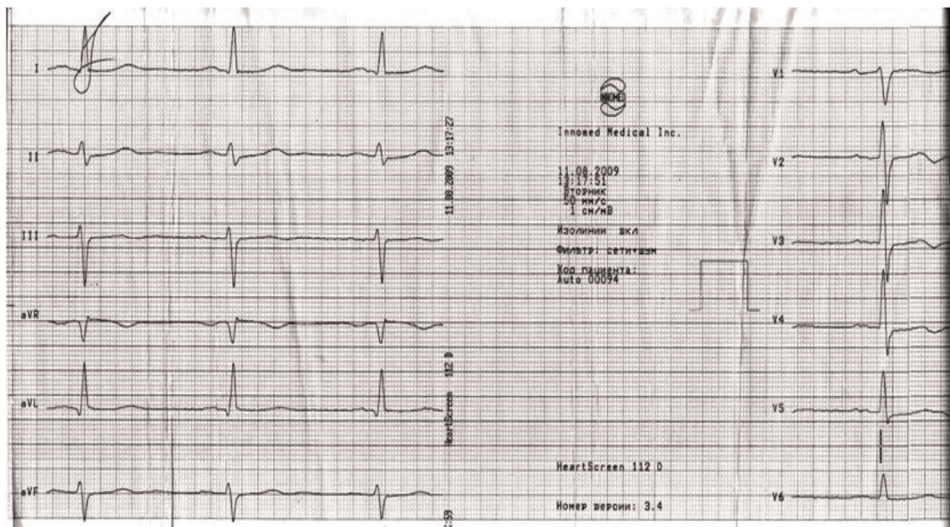
Analyzing the possibilities of using different methods for myocardial ischemia detection, it is necessary to take into account their position on the steps of the “ischemic cascade”. For example, systolic myocardial dysfunction, which is detected by echocardiography under load, in the ischemic cascade manifests itself later than the heterogeneity of blood flow. Manifestation of myocardial ischemia in the form of changes in the ST segment on the ECG is manifested even later and therefore the possibilities of the ECG in the detection of myocardial ischemia, even under load, are limited. At the top of the ischemic cascade is the anginal syndrome. What is the place of the MCG in this context? In our opinion, in some cases, the ICG at rest is outside the ischemic cascade, recording the “history” of episodes of past myocardial ischemia that have occurred before. The rather high sensitivity of the MCG is due to the fundamental physical advantages of the method. The rather high values of diagnostic accuracy of MCG received in numerous research are reached at rest. The causes of electrophysiological changes at rest in patients with coronary heart disease are diverse. First of all, these are changes in repolarization as a result of apoptosis. Also, previous episodes of myocardial ischemia can lead to cell necrosis in limited areas of the myocardium, causing impaired electrogenesis. Several articles have shown that transient ischemia contributes to an increase in interstitial endocardial fibrosis in patients with a history of MI. It is also suggested that in coronary heart disease already at rest there is a significant alternative to the level of myocardial blood supply. This in turn can also lead to subtle electrophysiological changes that are already taking place at rest.

It is known that myocardial ischemia is accompanied by activation of free radical processes, and it is obvious that this should be manifested by disturbances in the functioning of ion channels, changes in TPD, and excitability of conductive cells and cardiomyocytes. It can be assumed that changes in MCG parameters in patients with coronary heart disease at rest are due to changes in electrophysiological characteristics such as resistance of membranes and intercellular connections, and the rate of conduction.

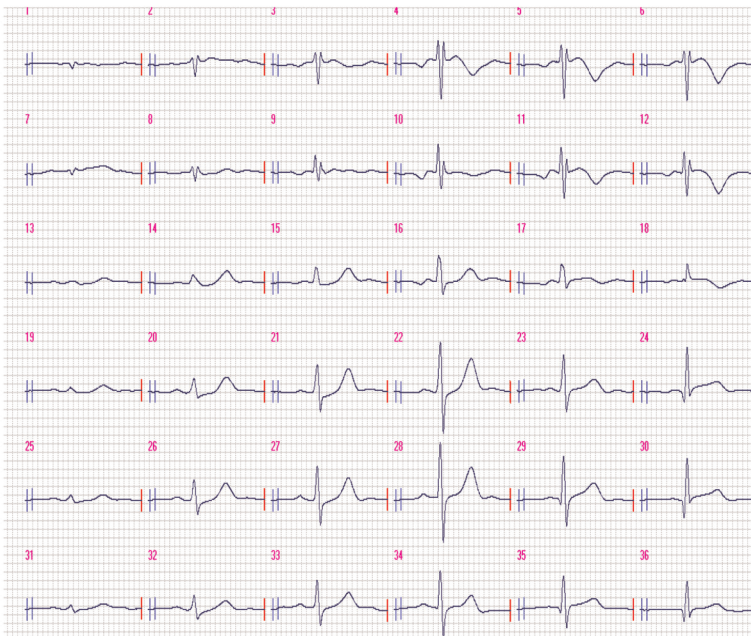
That is, we can conclude that due to its high sensitivity, the MCG at rest reveals the effects of episodes of transient ischemia (apoptosis, interstitial fibrosis, inhomogeneity of perfusion, and metabolism) [13].

Sufficiently high sensitivity of MCG is caused by fundamental physical advantages of the method. The result of these physical advantages is that the MCG signal more completely and accurately reflects electrical processes of the heart. MCG is much more sensitive than ECG to myocardial ischemia, thus MCG signal is changed even in cases when the shape of the ECG signal does not differ from normal. This advantage of MCG most clearly could be demonstrated by the shift of ST-segment (**Figure 14**).

Figure demonstrates standard ECG and MCG, registered on the same day almost simultaneously. There are no ST-segment shifts registered in any of the ECG leads. On the contrary, at points 14 and 20, there is a depression of ST-segment, and at points 4,5, and 6—an elevation of it.



(a)



(b)

Figure 14. ECG in 12 leads (A) and MCG (B) of the patient with 2 vessels CAD (high-grade RCA and LCX stenosis).

It is important to understand that the presence of depression and elevation simultaneously within the 36-point MCG grid has the same electrophysiological basis as reciprocal changes in ST-T interval of ECG leads. In the case above, there is an ST depression in the right-central quadrant of grid (points 14,20) and elevation in left-upper quadrant of MCG grid. In our opinion, this configuration may reflect ischemia of the inferior wall of the left ventricle. Naturally, the identified dislocations of the ST

segment will clearly appear on the CDV maps throughout this segment. We have developed the atlas of representative current density maps within ventricular repolarisation we have seen in patients with different variants of chronic CAD. We have selected “difficult-to-diagnose” patients with normal or uncertain, non-specific results of the routine tests. In that way, we would like we wanted to highlight the role of MCG in clinical routine—to feel out the gap between routine but non-sensitive diagnostic methods and much more expensive advanced non-invasive and invasive techniques [14].

8. Metrics and information technologies for the analysis of magnetocardiographic data based on three-dimensional visualization of the solution of the inverse problem

The original advanced method to solve the inverse problem of magnetostatics based on the results of measurements of the magnetic heart signal was developed recently. As the first step, a model of a point source of magnetic field (i.e., magnetic dipole) was used. The location and magnetic moment vector of magnetic dipole uniquely defined by known (measured) values of magnetic field at given points in space [15]. In the subsequent stages of data processing and conversion, other models of the signal source are also used. For example, the source of the magnetic field can be represented as a set of N different magnetic dipoles distributed in the volume of the heart [16]. In this case, the results of measurements of the magnetic field to determine the location of several signal sources are distributed as independent in the three-dimensional volume of the human heart. A model of a flat system of “currents” (distribution of the current density vector) is used for spatial analysis of the magnetic cardio signal and its sources. It is assumed that in space the selected plane, which is parallel to the plane of measurement, is secant with respect to the volume of the heart and is located at a given distance from the plane of measurement. In the proposed Primin and Nedayvoda algorithm, the coordinate of the plane with signal sources is a variable and its value is also determined by the measurements of the magnetic field—as the value of the z -th coordinate of the dipole source, which was determined at the previous stage of MCG signal processing. The problem for a planar current system is based on the application of the double integral Fourier transform and takes into account the spatial configuration of the magnetic flux transformer SQUID gradientometer [17]. An algorithm for converting information to solve the inverse problem was developed in the case if the results of measurements of the magnetic cardio signal need to determine the values of current density vectors in a given set of slices (“layers”) [18]. Each of the layers is located in a plane parallel to the measurement plane, the coordinates (“depth”) of each layer are set either with a given step (uniform distribution) or discretely based on the results of solving the inverse problem obtained in the previous stages (non-uniform distribution).

The power distribution of the current density vector is presented in the form of a so-called polar diagram. The principle of plotting is based on the segmentation scheme adopted as a standard in the analysis of measurement results in computed tomography and ultrasound of the heart [19]. Software implementation assumes that the three-dimensional surface consists of 5 segments: 1—anterior, 2—lateral, 3—inferior, 4—septal, and 5—apical.

Three-dimensional imaging methods have been successfully used to solve several important clinical problems, including, for example, determining the viability of the

affected areas of the myocardium in patients with various forms of coronary heart disease. Thus, a fairly high level (74%) was found between the contractility of the segments of the anterior wall of the left ventricle and the current density in this area of the myocardium in patients with chronic coronary heart disease [20].

9. Myocardial damage in patients recovered from COVID-19

2 years ago, a new challenge for humanity emerged—Covid-19 pandemic. It has led to well over 200 million infections, with a fatal outcome in over 4.5 million cases. Of the survivors, the majority showed long-haul symptoms – now often called Long COVID [21].

One of the important long-term clinical consequences of COVID-19 seems to be heart damage [22]. Signs and symptoms of possible heart damage after COVID-19 may include severe fatigue, palpitations, chest pain, shortness of breath, and postural orthostatic tachycardia syndrome (POTS) due to neurologic disturbances, post-exertional fatigue, and higher troponin levels.

In addition, heart inflammation appears to be prominent in COVID-19. This might involve both the myocardium and the pericarditis, causing severe fatigue without other obvious symptoms. The diagnosis of myocarditis is relatively inaccurate because both tests and diagnostic protocols are lacking precision. The course of the illness is therefore unknown at present, but some early reports have shown that symptoms lingered for a median of 47 days before diagnosis was accomplished by cardiac magnetic resonance (CMR) imaging [23].

Magnetocardiography, due to its high sensitivity is a potentially valuable method to detect the signs of myocardial damage in patients with COVID-19.

Therefore, 59 patients (mean age 42 ± 3.9 years) who recovered from COVID-19 were examined as it was shown in section 2 of this chapter in the Main Military Hospital of Ukraine and in the 8th People’s Hospital of Guangzhou. This group was divided into two subgroups depending on the time elapsed since recovery: 1–3 months after recovery (11 patients) and 7–10 month after recovery (48 patients). 78 healthy volunteers constituted the control group. These persons were examined earlier, in 2017–2018.

The method of data analysis was based on pattern recognition (see section 5 of this chapter). The probabilities of CDV maps within ST-T interval belonging (i.e., correlation coefficients) to six basic databases of reference images have been calculated. Each of these databases includes maps that are most specific to a particular disease. Then, the rank of category called “Non-coronary Heart Diseases” was determined. This rank (i.e., the relative value of the correlation coefficient) could be from 1 to 6.

To evaluate the difference between the examined groups, non-parametric Wilcoxon—Mann—Whitney test, designed to assess categorical variables, was used (Table 2).

There is a highly statistically significant difference between the rank of CDV maps, which belongs to the category “Non-coronary Heart Diseases” between the group of

Patients, recovered from COVID-19, total M±m, n = 59	1–3 month after recovery M±m, n = 11	7–10 month after recovery M±m, n = 48	Control group M±m, n = 78
3.78 ± 1.46 [*]	2.27 ± 1.67 [*]	4.08 ± 1.42	4.43 ± 1.25

^{*} $p \leq 0.05$ in comparison with control group.

Table 2.
The rank of category “Non-coronary Heart Disease” in groups examined.

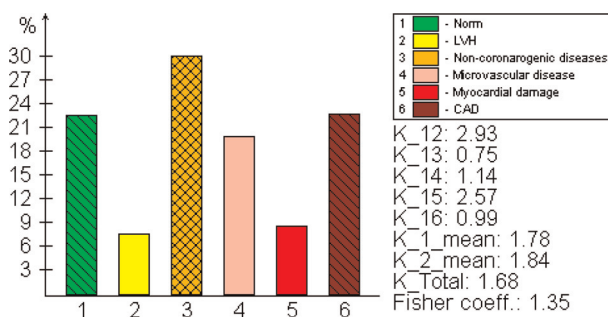


Figure 15.
 A diagram, showing the average correlation coefficients of CDV maps with 6 basic databases of reference images in a 61-years patient who has recently recovered from COVID-19. The highest correlation with the “Non-coronary Heart Diseases” category is observed.

patients recovered from COVID-19 and the control group. In patients, who recovered from COVID the signs of non-coronary heart diseases are much more pronounced, than in the control group. This is especially true for recently recovered patients, within 1–3 months before MCG-examination (**Figure 15**).

At the same time, the differences between the group of patients, who recovered from covid relatively long ago and the control group take place only at the level of a tendency ($p \leq 0.25$).

Note that all examples of the application of the new metric for the analysis of subtle changes in the magnetic field of the human heart are critical parts of the relevant new diagnostic technologies.

The meaning of the development and implementation of any new diagnostic technology is to solve difficult diagnostic problems that are difficult to solve with existing methods. The above examples of new metrics developed by us fully meet the criteria for solving a complex diagnostic problem in cardiology, and in the first place, there is a wide range of differential diagnosis and low availability and/or high cost of diagnostic methods already included in existing clinical guidelines on this problem. In addition, it should be noted that a key sign of the maturity of the new technology is the presence of certificates of conformity issued by the authorized department of a country, as well as patents confirming its novelty. In this context, it should be noted that in addition to national certificates and patents, our proposed metrics as a result of careful long-term testing of the most modern procedures and received the relevant international certificates and patents for inventions. This is a guarantee of further intensive use of the unshielded magnetocardiography in medical practice at the international level.

The emerging diagnostic technology regarding existing ones might play one of the three future roles: replacement, triage or adds one [24]. At present, magnetocardiography can play the role of triage and supplementation among well-established methods for diagnosing myocardial damage of various origins. Further development of the method requires further, larger multicenter studies involving several dozen clinics in different countries.

10. Conclusions

1. The development of new information technologies and metrics based on magnetocardiography for the analysis of small changes in biological signals is a

modern technological trend that improves the accuracy of many diagnostic methods, including methods of analysis of electrical activity of the heart.

2. New magnetocardiographic metrics for the analysis of the spatial structure of 2D magnetocardiographic current density distribution maps allow to diagnose myocardial ischemia with high accuracy, which has been proven in the course of intercenter studies.
3. Metrics based on three-dimensional visualization (polar diagram) of the electrical activity of the ventricles of the heart on the basis of magnetocardiographic data provide an opportunity to solve important clinical problems, in particular to determine the viability of affected myocardial infarction in patients with various forms of coronary heart disease.
4. New metrics for 2D magnetocardiographic current density distribution maps analysis, based on pattern recognition allow to detect signs of myocardial damage in patients, who recently recovered from COVID-19. Further, larger studies are needed to confirm these findings.

Acknowledgements

The authors want to express their sincere gratitude to outstanding experts in physics, mathematics, cryogenic engineering Drs. Michael Primin, Volodymyr Sosnytskyy, Pavlo Sytkovy, Igor Nedayvoda, Yury Minov, Pavlo Shpylevoi, Mykola Budnyk, Yury Frolov from Glushkov Institute for Cybernetics of NAS of Ukraine as well as Dr. Anton Popov and Eugen Udovichenko from National Technical University of Ukraine “Igor Sikorsky Kyiv Polytechnic Institute”. In addition, the authors warmly thank the great teams of leading hospitals in Ukraine, China, and Germany, with whom they were lucky to productively cooperate.

Special thanks to Mr. Bin-Zhen Zhang from North University of China, Mrs. Wei-Wei Quan from Ruijin Hospital affiliated to Shanghai Jiaotong University, as well as Mrs. Xiang-Yan Kong from Ningbo University for their outstanding efforts aiming to develop MCG-technology in China.

Author details

Illya Chaikovsky^{1*}, Anatoly Kazmirchyk², Sergey Sofienko², You-Bin Liu³,
Ya-Feng Zhou⁴, Xie Feng⁵, Lin Xu⁵ and Yan-Fei Huang⁵

1 Glushkov Institute for Cybernetics, Kiev, Ukraine

2 National Military Medical Clinical Center (MMCH), Kiev, Ukraine


3 8th People's Hospital of Guangzhou, Guangzhou, China

4 Suzhou Dushu Lake Hospital, Suzhou, China

5 Suzhou Cadiomox Ltd, Suzhou, China

*Address all correspondence to: illya.chaikovsky@gmail.com

IntechOpen

© 2022 The Author(s). Licensee IntechOpen. This chapter is distributed under the terms of the Creative Commons Attribution License (<http://creativecommons.org/licenses/by/3.0>), which permits unrestricted use, distribution, and reproduction in any medium, provided the original work is properly cited. 

References

- [1] Benjamin EJ, Virani SS, Callaway CW, Chamberlain AM, Chang AR, Cheng S, et al. Heart disease and stroke statistics–2018 update: A report from the American Heart Association. *Circulation*. 2018;**137**(12): 67-492
- [2] Simoons ML, Hugenholtz PG. Estimation of the probability of exercise induced ischemia by quantitative ECG analysis. *Circulation*. 1977;**56**:552-559. DOI: 10.1161/01.CIR.56.4.552
- [3] Gerhard B, Richard M. Detection of the magnetic field of the heart. *American Heart Journal*. 1963;**66**(1):95-96
- [4] Chaikovsky I, Lutay M, Sosnitsky V, et al. Ventricular repolarization disturbances diagnostics in chronic ischemia patients evidence derived from MCG. In: *Biomag 96: Proc of 10th International Conference on Biomagnetism*. 1999. pp. 444-447
- [5] Chaikovsky I, Kohler L, Hecker T, Hailer B. High sensitivity of magnetocardiography in patients with coronary artery disease and normal or unspecifically changed ECG. *Circulation*. 2001;**102**(18):791
- [6] Cohen D, Edelsack EA, Zimmerman JE. Magnetocardiograms taken inside a shielded room with a superconducting point-contact magnetometer. *Applied Physics Letters*. 1970;**16**(7):278-280. DOI: 10.1063/1.1653195
- [7] Koch H. Recent advances in magnetocardiography. *Journal of Electrocardiology*. 2004;**37**:117-122. DOI: 10.1016/j.jelectrocard.2004.08.035
- [8] Dutz S, Bellemann ME, Leder U, Haueisen J. Passive vortex currents in magneto- and electrocardiography: Comparison of magnetic and electric signal strengths. *Physics Medical Biology*. 2006;**51**(1):145-151
- [9] Chaikovsky I. Magnetocardiography in unshielded location in coronary artery disease detection using computerized classification of current density vectors maps. 2006
- [10] Udovychenko Y, Popov A, Chaikovsky I. Multistage classification of current density distribution maps of various heart states based on correlation analysis and k-NN algorithm. *Frontiers in Medical Technology*. 2021:3-11
- [11] Udovychenko Y, Popov A, Chaikovsky I. k-NN binary classification of heart failures using myocardial current density distribution maps. In: *Signal Processing Symposium (SPSymo)*. 2015. pp. 98-102
- [12] Chaikovsky I, Hailer B, Sosnytskyy V, Lutay M, Mjasnikov G, Kazmirchuk A, et al. Predictive value of the complex magnetocardiographic index in patients with intermediate pretest probability of the chronic CAD: Results of a Two-Center Study. *Coronary Artery Disease*. 2014;**25**(6):474-484. DOI: 10.1097/MCA.000000000000107
- [13] Buja LM, Entman ML. Modes of myocardial cell injury and cell death in ischemic heart disease. *Circulation*. 1998;**98**:1355-1357. DOI: 10.1161/01.CIR.98.14.1355
- [14] Chaikovsky I, Auth-Eisernitz S, Avolin B, et al. Atlas of typical magnetocardiographic maps for diagnosis of CAD within ST-T interval. In: *Proc. of 14th International Conference on Biomagnetism, Boston*. 2004. pp. 393-394

- [15] Primin M, Nedayvoda I. Mathematical model and measurement algorithms for a dipole source location. *International Journal of Applied Electromagnetics and Mechanics*. 1997; **8**(2):119-131
- [16] Primin M, Nedayvoda I. Inverse problem solution algorithms in magnetocardiography: New analytical approach and some results. *International Journal of Applied Electromagnetics and Mechanics*. 2009; **29**(2):65-81. DOI: 10.3233/JAE-2009-1001
- [17] Primin MA, Nedayvoda IV. A method and an algorithm to reconstruct the spatial structure of current density vectors in magnetocardiography. *Cybernetics and Systems Analysis*. 2017; **53**(3):485-494. DOI: 10.1007/s10559-017-9950-6
- [18] Primin M, Chaikovskiy I, Berndt C, Nedayvoda I. Layer-to-layer heart electrical image based on magnetocardiography data in comparison with perfusion image based on PET. *International Journal of Bioelectromagnetic*. 2003; **5**(1):27-28
- [19] Cerqueira MD, Weissman NJ, Dilsizian V, Jacobs AK, Kaul S, Laskey WK, Pennell DJ. Standardized myocardial segmentation and nomenclature for tomographic imaging of the heart. A statement for Healthcare Professionals from the Cardiac Imaging Committee of the Council on Clinical Cardiology of the American Heart Association. *Circulation*. 2002; **105**(4): 539–542. DOI: 10.1067/mnc.2002.123122
- [20] Chaikovskiy I, Primin M, Nedayvoda I, Mjasnikov G, Kazmirchik A, Lutay M, et al. Monitoring of myocardial viability in patients with myocardial infarction based on magnetocardiographic analysis of ventricular depolarisation. *Journal of the American College of Cardiology*. 2018; **72**(16):C89. DOI: 10.1016/j.jacc.2018.08.475
- [21] Callard F, Perego E. How and why patients made Long Covid. *Society Science Medicine*. 2021; **268**:113426
- [22] Metkus TS, Sokoll LJ, Barth AS, Czarny MJ, Hays AG, Lowenstein CJ, et al. Myocardial injury in severe COVID-19 compared with non-COVID-19 acute respiratory distress syndrome. *Circulation*. 2021; **143**:553-565. DOI: 10.1161/CIRCULATIONAHA.120.050543
- [23] Puntmann VO, Carerj ML, Wieters I, et al. Outcomes of cardiovascular magnetic resonance imaging in patients recently recovered from coronavirus disease 2019 (COVID-19). *JAMA Cardiology*. 2020; **5**(11):1265-1273. DOI: 10.1001/jamacardio.2020.3557
- [24] Bossuyt PM, Irwig L, Craig J, Glasziou P. Comparative accuracy: Assessing new tests against existing diagnostic pathways. *British Medical Journal*. 2006; **332**(7549):1089-1092

Edited by Umashankar Lakshmanadoss

This book provides a comprehensive overview of electrocardiogram (ECG), including both the electrophysiological aspects of ECG and how to identify common diseases like coronary artery diseases based on ECG. This book is divided into two sections: “Practical Applications of ECG in Arrhythmias” and “Clinical Use of ECG”. Chapters address such topics as an interpretation of intra-cardiac ECG during electrophysiology study, classic ECG features of narrow and wide QRS complex tachycardias, use of ECG in cattle, and use of unshielded magnetocardiography to detect myocardial damage in patients recovering from COVID-19.

Published in London, UK

© 2023 IntechOpen
© evryka23 / iStock

IntechOpen

